Mitt. österr. geol. Ges.	84 (1991)	S. 265-300 39 Abb., 4 Tab.	Wien, Juni 1992

Paragenesis of Complex Massive Sulfide Ores from the Tyrrhenian Sea

By Werner TUFAR*)

With 39 Figures and 4 Tables

Zusammenfassung

Eine herausragende Stellung innerhalb der heutigen Geowissenschaften nimmt die Untersuchung der rezenten hydrothermalen Aktivität und Lagerstättenbildung an aktiven Spreizungsrücken ein, nämlich die rezenten Komplexmassivsulfiderz-Mineralisationen („Schwarze Raucher") an divergierenden Plattenrändern (z. B. Ostpazifischer Rücken) sowie an Spreizungsrücken in Back-Arc-Becken (z. B. Manus-Becken/Bismarck-See — Papua-Neuguinea). Eine rezente Komplexmassivsulfiderz-Mineralisation ist mittlerweile auch vom Tiefseeberg Palinuro aus dem südöstlichen Tyrrhenischen Meer, nördlich von Sizilien und den Liparischen Inseln, bekannt. Am Tiefseeberg Palinuro tritt in cirka 630 m Wassertiefe eine sehr komplexe Massivsulfiderz-Mineralisation auf, die aus Sulfiden, Sulfosalzen und Sulfat-Gangart besteht. Als ein Charakteristikum zeichnet sich die Paragenese durch hohe Gehalte an Bleiglanz und Baryt aus. Weitere Hauptgemengteile bilden Pyrit, Melnikovitpyrit, Zinkblende und Schalenblende, Nebengemengteile u. a. Markasit, Enargit und Kupferkies, Akzessorien z. B. Tennantit, Bravoit, Covellin sowie ein weiteres Sulfosalz, vermutlich Jordanit. Das Auftreten von Enargit und Tennantit läßt ersehen, daß eine eisenarme Buntmetall-Mineralisation vorliegt. Die Erzmineralisation ist außerdem durch sehr hohe Spurengehalte an Quecksilber (max. 0,67 %) gekennzeichnet. Interessante Spurenkonzentrationen liegen auch bei den Edelmetallen Silber und Gold vor. Die auftretenden Verwachsungen sind häufig feinkörnig ausgebildet. Vielfach liegen komplexe rhythmische Abfolgen vor, Kolloidalgefüge bzw. Geltexturen sind verbreitet. Plastische, sedimentäre Deformation und Faltung von Erzlagen machen auf das Vorliegen eines ursprünglich unverfestigten Erzschlammes aufmerksam. Typisch für die Erzmineralisation sind häufig anzutreffende diagenetische Gefüge, die besonders eindrucksvoll von Bleiglanz abgebildet werden. Eine weitere Besonderheit des Vorkommens stellen im Komplexmassivsulfiderz erhaltene bzw. pseudomorphosierte laminierte Matten von Mikroorganismen dar, wahrscheinlich liegen Bakterien-Matten vor. Paragenetische Vergleiche der Komplexmassivsulfiderze vom Tiefseeberg Palinuro können mit bekannten „fossilen" syngenetischen Buntmetall-Lagerstätten durchgeführt werden, z. B. mit der Lagerstätte Veovača in Bosnien.

Summary

In the geosciences of our time, the investigation of modern hydrothermal activity and the metallogenesis of active spreading centers occupies a distinctive position. Particularly interesting examples are the modern complex massive sulfide mineralizations ("black

*) Author's address: Prof. Dr. Werner TUFAR, Fachbereich Geowissenschaften der Philipps-Universität Marburg, Hans Meerwein-Straße, D-3550 Marburg/Lahn, Germany

smokers") at actively spreading plate boundaries (e. g. the East Pacific Rise) and also at spreading ridges within back-arc basins (e. g. the Manus Basin/Bismarck Sea, Papua New Guinea). A modern complex massive sulfide mineralization is in the meantime also known from the Palinuro Seamount in the southeastern part of the Tyrrhenian Sea, north of Sicily and the Lipari Islands. At the Palinuro Seamount a complex massive sulfide formation occurs at water depths near 630 m. The paragenesis is characterized by sulfides, sulfosalts and sulfate gangue material. Major mineral constituents are pyrite, melnikovite-pyrite, sphalerite, schalenblende, galena and barite. Minor mineral components are enargite and chalcopyrite. Enargite and the accessory components tennantite, bravoite, covellite and another sulfosalt, probably jordanite, indicate an Fe-poor non-ferrous metal paragenesis. Among other things, this is also characterized by a considerable concentration of Hg (maximum 0.67 %) and substantial traces of Ag and Au. The intergrowths of the ore minerals are often very fine-grained and frequently complex paragenetic successions and rhythmic alternations are documented. Moreover, typical colloidal and/or gel textures are very common. In places, slumping (slump bedding) can be observed within the sulfide layers, indicating an ore mud origin. Furthermore, characteristic sulfide textures (e. g. galena) reveal the later influence of diagenesis. The occurrence of galena as a typical major mineral constituent in this complex massive sulfide mineralization already reveals the influence of portions of the continental crust as a source for the leaching hydrothermal solutions. A further particular feature of this mineralization is the presence of microbial mats, presumably laminated bacterial mats, which are preserved within and pseudomorphed by this complex massive sulfide ore. By comparison, the complex massive sulfide formation at the Palinuro Seamount exhibits paragenetic relationships and textures which can also be observed in well-known ancient ("fossil") syngenetic base metal deposits on the continents (e. g. in Bosnia).

Contents

1. Introduction

Massive sulfide occurrences in a modern seafloor environment are of particular significance. Active divergent plate boundaries with areas of intense hydrothermal activity giving rise to the formation of ore deposits are of major importance. They have received a lot of attention from geoscientists in recent years. The East Pacific Rise and the Galápagos Rift are especially suited for the study of such processes.

Hydrothermal activity at modern seafloor spreading centers is a prime target for the study of mechanisms leading to the formation of massive sulfide mineralizations.

Hydrothermal mineralizations from the Tyrrhenian Sea were reported by M. MINITTI and F. F. BONAVIA (1984), who focussed attention on the occurrence of sulfide ores in this part of the Mediterranean Sea.

The recovery of massive sulfides from the Palinuro Seamount in the Tyrrhenian Sea during the SO 41 — HYMAS I Research Cruise ("**Hy**drothermale **Mas**sivsulfide" — hydrothermal massive sulfides) with the German Research Vessel Sonne is considered a major success (Station SO 41-181 FG). Sulfide clumps embedded in sediment were found at a water depth of 630 m (Fig. 1).

No active hydrothermal venting was found at the Palinuro Seamount. However, indications for modern hydrothermal activity could be observed in the neighborhood of the sulfide occurrence.

Information about this sulfide mineralization has been presented by D. LASCHEK (1986), H. PUCHELT (1986), H. PUCHELT and D. LASCHEK (1987), P. STOFFERS and G. C. AMSTUTZ (1987), W. TUFAR (1990 a, 1991), and W. TUFAR et. al. (1987).

2. Sample Description

All sulfide ore specimens consist of complex massive sulfide assemblages. Macroscopically, sample fragments exhibit porous, occasionally banded or crustaceous to rhythmically layered textures. Found in association with sulfides is the gangue material barite, which locally shows a considerable enrichment.

2.1. Complex Massive Sulfides

Chemical analyses (Table 1-4) of the complex massive sulfide ore samples show mostly high concentrations of zinc, iron and especially barium, substantial to high contents of lead in particular, and only low concentrations of copper. Concerning the trace elements, significant concentrations of arsenic, antimony, cadmium and molybdenum are of particular interest. Very conspicuous are extremely high trace concentrations of mercury. Substantial traces of the precious metals silver and gold are also conspicuous.

A thorough study of massive sulfides by means of ore microscopy is considered particularly useful for the characterization of the mineralogically complex suite. Such a study provides detailed information about the present ore minerals, their intergrowths and genesis and, with regard to the economic potential of the deposit, yields important parameters for process mineralogy and metallurgy.

The porous, partially layered and/or crustaceous textures of the specimens already observed on a macroscopic scale is also evident microscopically.

Volumetrically, the amount of individual sulfide minerals varies considerably between different specimens. Pyrite, sphalerite, schalenblende, and galena are major ore components, although their relative proportions vary strongly. Melnikovite-pyrite constitutes either a major or a minor component. Minerals such as "intermediate product", marcasite, chalcopyrite, and enargite represent minor constituents, while wurtzite, covellite, bravoite, tennantite, and a lead-sulfosalt, probably jordanite, occur less frequently.

Colloidal and/or gel textures (colloform textures) are typical of the sulfide association (Figs. 2-10, 12-17, 19-23, 26-28, 30-33, 38). Rhythmic colloform, colloidal masses are in many instances excellently displayed by pyrite, melnikovite-pyrite, "intermediate product", schalenblende, and galena. These portions take the form of rhythmically layered, botryoidal to reniform, concentrically layered, or orbicular to radial masses.

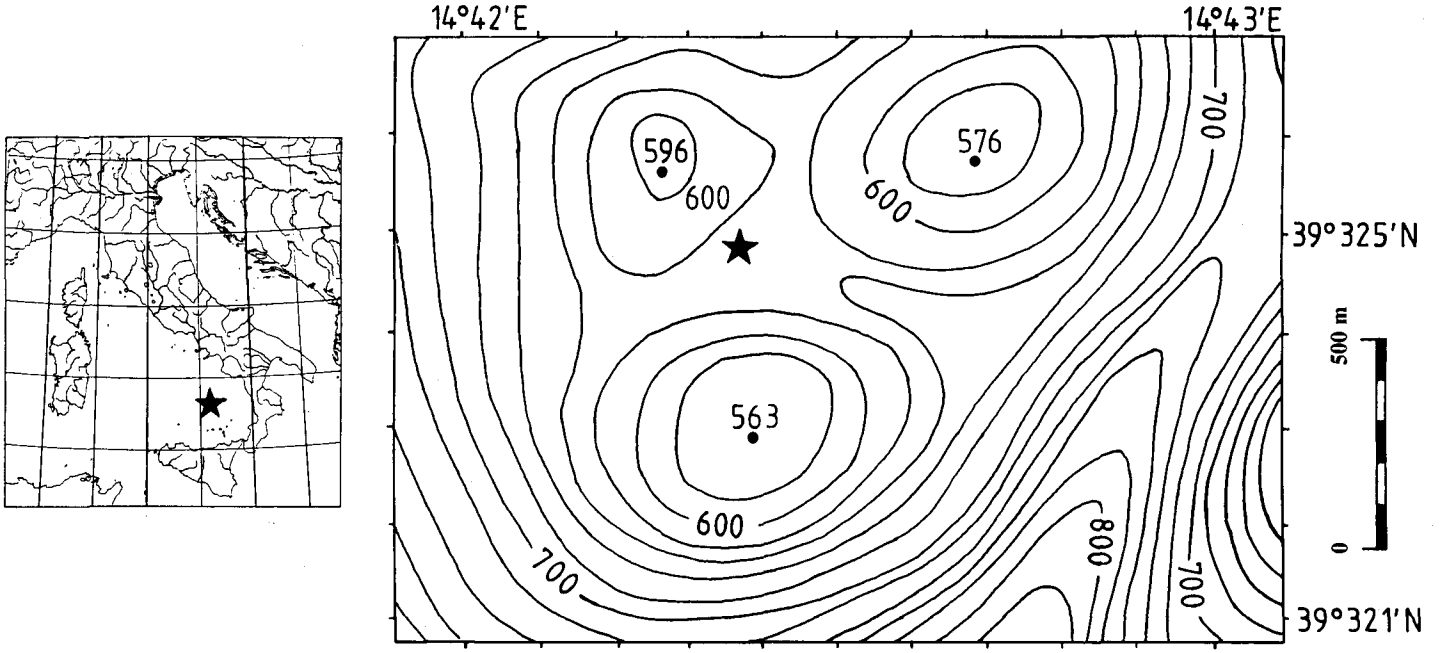

Fig. 1. Bathymetric map of the Palinuro Seamount showing the sampling location of the complex massive sulfide mineralization. (Water depths are in meters, 20 meter contour intervals)
(After H. PUCHELT, 1986).

Pyrite (Figs. 2-7, 9-38) forms a major mineral constituent, mostly found in rhythmic, colloidal masses, usually in association with schalenblende, sphalerite, galena, and melnikovite-pyrite and, to a lesser extent, associated with "intermediate product" and marcasite. Sporadically, pyrite exhibits differences in its reflectivity where a less strongly reflecting **brown variety** occurs. The latter may be distinguished from locally present bravoite. Pyrite is often found in abundance as very finely disseminated inclusions in other sulfides, such as schalenblende and sphalerite. Furthermore, pyrite is encountered as an overgrowth on, occasionally even as interstitial filling in, or rim around, adjacent aggregates of sphalerite or galena. Pyrite entirely encloses the latter two in places. Locally, when occurring peripherally and interstitially to schalenblende or as a rim around galena, pyrite itself is rimmed by bravoite (Figs. 16, 26-28). Inclusions of sulfides (schalenblende, sphalerite, galena) and gangue material (tabular barite) are common in pyrite. The mineral quite often reveals its euhedral form, though usually very fine-grained.

In places, bubble-like spheroids exhibiting a mostly thick superficial shell of pyrite (Figs. 4-5, 30) occur frequently. These typical spheroids often display a center consisting of gangue material, frequently barite, which in many cases exhibits crystal aggregates. Shrinkage cracks are common, both in the gangue material occupying the center and in the thick superficial shell of pyrite. These shrinkage cracks can be healed and cemented by galena and pyrite itself.

Furthermore, smaller spheroids composed of concentrically layered pyrite are encountered occasionally (Figs. 2, 7, 9-10, 12-14, 16-17, 21). In addition framboidal pyrite (Fig. 3) occurs locally in association with minute, loosely packed crystal aggregates of porous

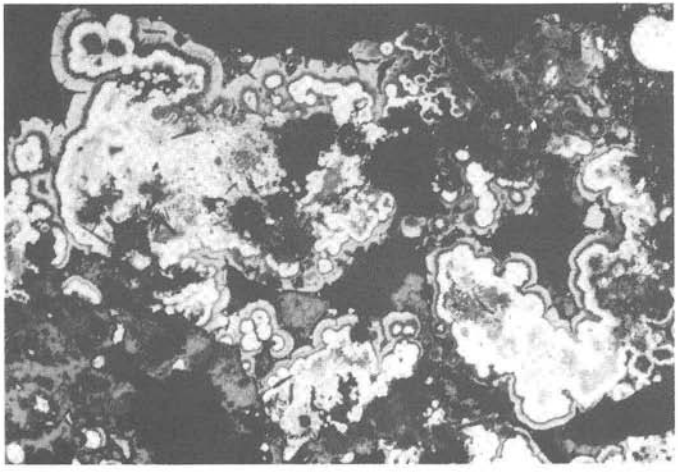

Fig. 2. Sample SO 41-181 FG 7.
Excellent colloidal masses of rhythmically layered to concentric pyrite (light gray, almost white), melnikovite-pyrite (medium gray to dark gray), and "intermediate product" (likewise medium gray to dark gray) as well as interstitial and peripheral schalenblende (dark gray) contain tiny euhedral plates and crystal aggregates of barite (black) in places. Locally shrinkage cracks occur in melnikovite-pyrite and "intermediate product". There is a pyrite spheroid in the upper right corner. Gangue material, abundant natural cavities and pores (all likewise black).
Polished section, ×85.

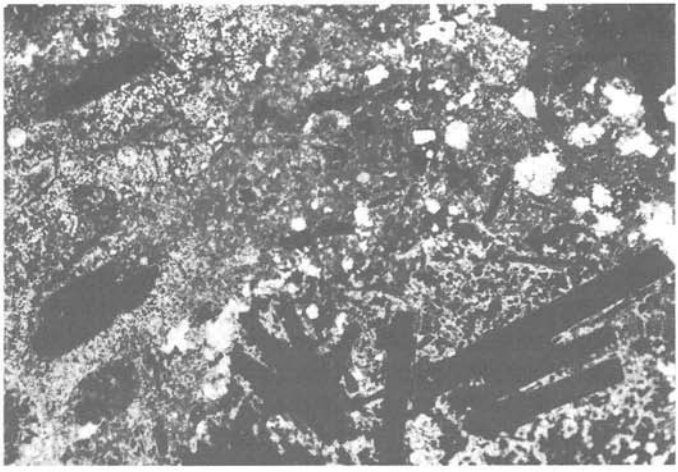

Fig. 3. Sample SO 41-181 FG 13.
Delicate, rhythmically layered to concentric masses of schalenblende (dark gray) and galena (light gray) are associated with fine-grained pyrite (light gray, almost white) partly developed as framboidal pyrite. In interstices and pores massive pyrite and euhedral galena are encountered locally. Barite plates (black) of different size, euhedrally developed after {001}, are enclosed in the ore. Natural cavities and pores (all likewise black).
Polished section, oil immersion, ×275.

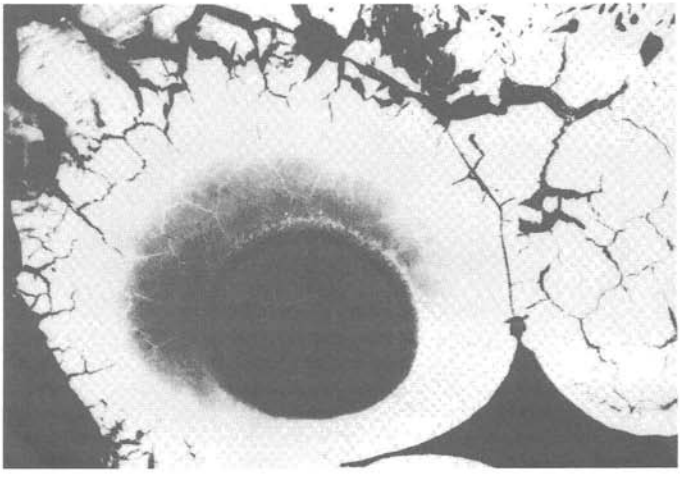

Fig. 4. Sample SO 41-181 FG 10.
Bubble-like spheroid, showing a center consisting of gangue material (black) followed by a broad superficial shell of pyrite (light gray, almost white). Within these spheroids, both gangue material and pyrite reveal impressive shrinkage cracks which in places are cemented by pyrite.
Polished section, oil immersion, ×65.

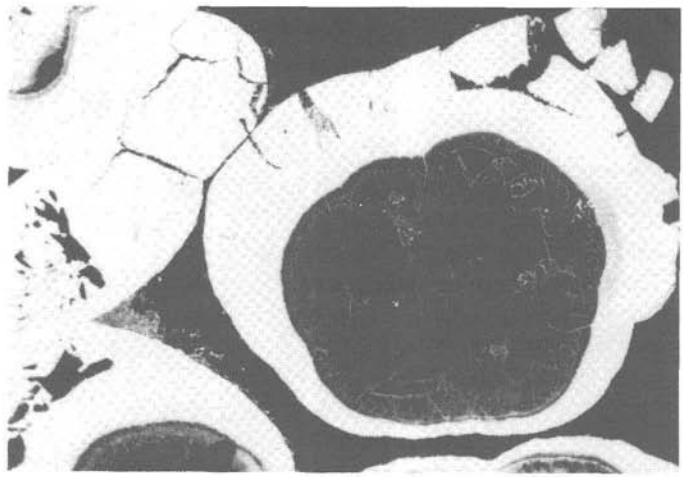

Fig. 5a.

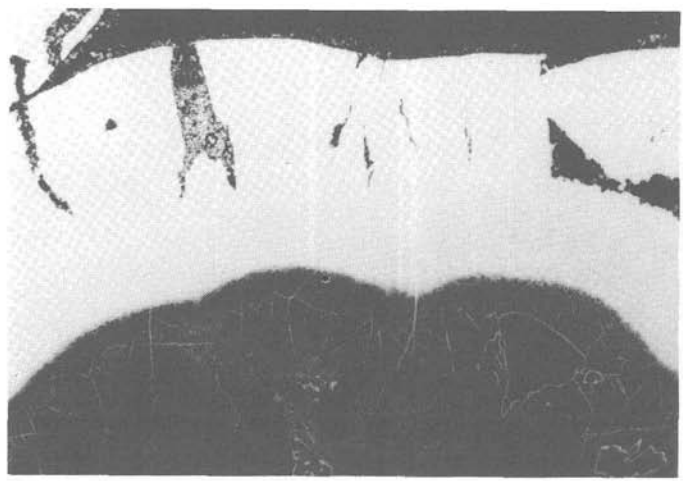

Fig. 5b.

Fig. 5. Sample SO 41-181 FG 10.
Bubble-like spheroids exhibiting typical shrinkage cracks within the center, composed of gangue material (black), as well as in the outer broad superficial shell, consisting of pyrite (light gray, almost white). The pyrite cements shrinkage cracks and fractures within the gangue material occupying the center and partly even within the outer rim of pyrite itself. Fine-grained, porous crystal aggregates of galena (light gray) also can be observed in places as fillings of shrinkage cracks in the peripheral parts of the gangue material occupying the center, there near the boundary to the outer superficial shell of pyrite, as well as in shrinkage cracks of the broad pyrite rim, peripherally around these rims and in interstices of the spheroids. Figure 5b demonstrates in impressive detail these charactersitic shrinkage cracks and their healing by pyrite and fillings by fine-grained, porous crystal aggregates of galena in the outer superficial shell of pyrite, as well as in the gangue material occupying the center of the bubble-like spheroid.
Polished section, oil immersion, Fig. 5a: ×65, Fig. 5b: ×160.

pyrite. Rather unique are occasional heterogeneous, euhedral aggregates (Figs. 20-22), predominantly consisting of fine-grained, distinctly euhedral pyrite in a "matrix" of enargite or of fine-grained, partially euhedral pyrite with chalcopyrite, minor sphalerite, galena, and enargite. Rims of enargite intergrown occasionally with subordinate sphalerite and minor bravoite usually cover these heterogeneous, euhedral aggregates. A further striking feature of the paragenesis is the sporadic myrmekitic intergrowth of pyrite and enargite (Figs. 11, 25).

Zinc sulfide (Figs. 2-3, 6-24, 26-27, 29, 32-38), another major ore component, occurs on the one hand as sphalerite, and on the other hand as schalenblende and wurtzite, although wurtzite was rarely encountered.

A primary origin of **sphalerite** is readily evident from its euhedral crystal aggregates, supported by the occurrence of polysynthetic twin lamellae.

Schalenblende is very commonly found in rhythmically layered crusts and botryoidal-reniform to concentrically layered colloform masses, exhibiting colloidal and/or gel textures.

Sphalerite and schalenblende show complex, alternating, in places extremely intimate intergrowths mainly with galena, pyrite, and melnikovite-pyrite. Likewise, the two zinc sulfides locally contain abundant zonal inclusions of other sulfides, in particular galena. These inclusions are commonly very fine-grained and chiefly composed of galena, which is disseminated in places. Rhythmic layering and alternations of galena, sphalerite, and/or schalenblende are commonly extremely minute and, as with the grain size of galena inclusions, approach dimensions close to the limit of optical resolution.

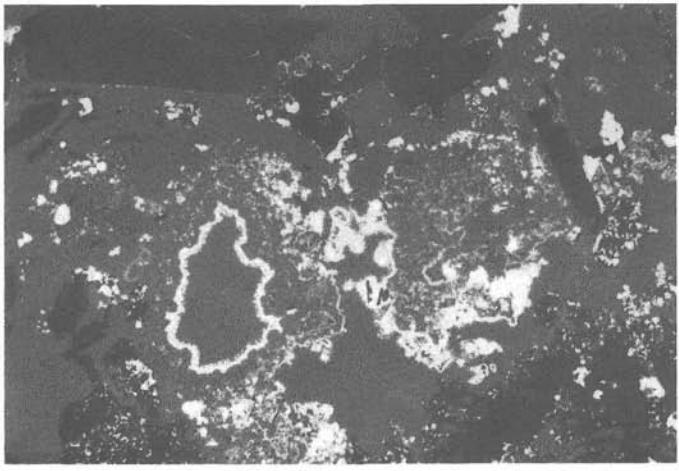

Fig. 6. Sample SO 41-181 FG 9.
Schalenblende (dark gray) frequently displays rhythmic, concentrically layered alternations with galena (light gray), which constitutes rims and fills interstices, there partly forming tiny crystal aggregates. Smaller and larger crystals of barite (black) are enclosed in schalenblende or in turn overgrow the latter. In places, coatings of galena ("intergranular films") or occasionally of schalenblende (upper left corner) occur around euhedral barite aggregates. Additionally, a small ammount of pyrite (light gray, almost white) is present locally. Gangue material, natural cavities and pores (all likewise black).
Polished section, oil immersion, ×165.

Tabular euhedral barite (Figs. 2-3, 6-7, 9-13, 15, 17, 19) is often found as an inclusion in sphalerite and schalenblende, both of which often form excellent interstitial fillings in crystal aggregates of barite and rims around them.

Very small differences in reflectivity of sphalerite and schalenblende occasionally delineate zoning. Variable iron contents seem to account for this property, as well as for irregularities in the intensity and color of internal reflections.

Local plastic deformation of rhythmic layers and alternating bands of mainly galena contained in sphalerite and schalenblende point to sedimentary slumping, while the ore mud was still in an unconsolidated state ("slump folding", "slumping" — Fig. 12).

Shrinkage cracks (Figs. 10-11) in sphalerite and schalenblende are conspicuous and filled with galena and pyrite, occasionally accompanied by covellite.

Galena, yet another major ore mineral (Figs. 3, 5-18, 20-24, 27-33, 38), forms aggregates of variable grain size, in part found finely intergrown with other sulfides, or occurs as inclusions in them.

When it occurs in rhythmic alternation with sphalerite and schalenblende, galena often displays well developed colloform, colloidal and/or gel textures, as in rhythmic to concentrically layered masses (Figs. 3, 6-8, 10, 12-13, 33). Alternating rhythmically layered crusts are small enough to approach the limits of optical resolution, just as with galena disseminated in sphalerite and schalenblende.

Frequently, euhedral galena crystal aggregates of various size (Figs. 3, 5-8, 11-18, 20-21, 23-24, 27-28, 30-33) are encountered. In these aggregates galena often constitutes an accretion, overgrowth, or rim and interstitial coating or filling, mainly in sphalerite and/or

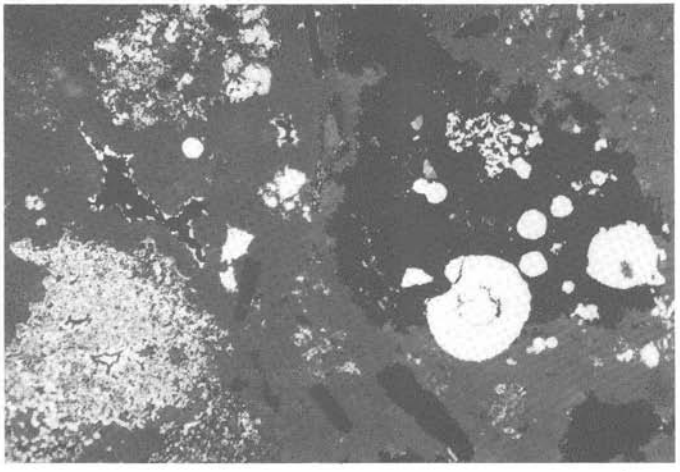

Fig. 7. Sample SO 41-181 FG 7.
Schalenblende (dark gray, internal reflections) comprises zonally arranged, delicate, rhythmic to concentrically layered alternations with galena (light gray). The latter mineral may also be observed in interstices as a fine-grained accretion, partially displaying euhedral development. In places, pyrite (light gray, almost white) develops its characteristic spheroids at the margins of schalenblende, in which it is also contained. Occasionally barite plates (black) occur. Gangue material, natural cavities and pores (all likewise black).
Polished section, oil immersion, ×275.

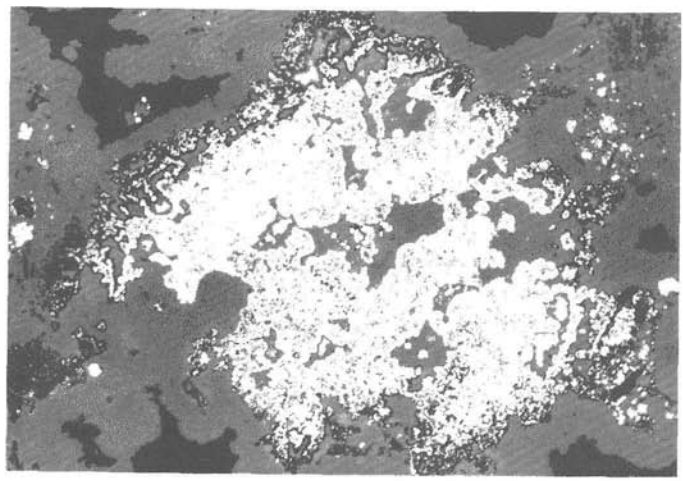

Fig. 8. Sample SO 41-181 FG 7.
Excellent, rhythmic to concentrically layered masses of schalenblende (dark gray, internal reflections) and galena (light gray, almost white). Interstices in schalenblende display accretion of and coating with galena. Gangue material, abundant natural cavities and pores (all likewise black).
Polished section, oil immersion, ×165.

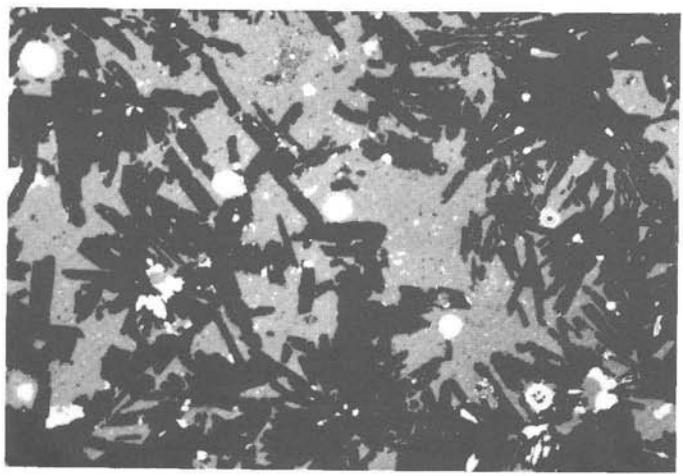

Fig. 9. Sample SO 41-181 FG 9.
Schalenblende (medium gray) encloses abundant crystal aggregates of barite (dark gray, almost black) euhedrally developed after {001} and, occasionally accompanied by pyrite (light gray, almost white), completely fills their interstices. Additionally the characteristic concentric spheroids of pyrite are embedded in schalenblende, which furthermore contains small inclusions of galena (light gray).
Polished section, ×165.

schalenblende, thereby locally forming inclusions in the zinc sulfides. Occasionally, fine-grained, loose to porous aggregates of galena display dendritic and "knitted" aggregates to crystal skeletons (Figs. 13, 18, 23, 28, 30-33), either in sphalerite and schalenblende or along their periphery. Euhedral galena aggregates, often accumulating around and overgrowing on other minerals themselves, are in turn enclosed in sphalerite and schalenblende (Fig. 17). Furthermore, galena exhibits local rims of pyrite (Figs. 15-17, 27), which in turn is enclosed in bravoite. The latter, as well as the adjoining pyrite, may be succeeded by a later generation of small euhedral galena. Locally, a later generation of galena forms a rim around earlier crystal skeletons of galena (Fig. 18).

In addition, galena is observed in delicate rims and intergranular coatings in and around sphalerite and tabular barite (Fig. 11). Partially coexisting with covellite, galena fills fractures and shrinkage cracks in sphalerite and schalenblende (Figs. 10-11). Rarely, crystal skeletons of galena are intimately intergrown with gangue material to constitute myrmekites (Fig. 18).

The plastic deformation of rhythmic, alternating layers of galena contained in sphalerite and schalenblende indicates deformation (slump folding, slumping) prior to diagenesis in the unconsolidated ore mud (Fig. 12). Diagenetic effects in galena are apparent also from accretions, overgrowth forms, interstitial fillings, healing and cementing of shrinkage cracks, etc. (Figs. 3, 5-8, 12-17, 20-23, 27-28, 30-33).

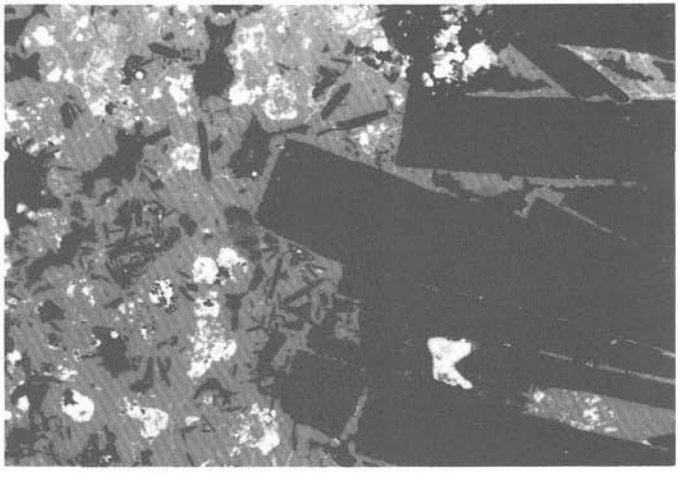

Fig. 10. Sample SO 41-181 FG 6.
Schalenblende (medium gray) encloses fine-grained, occasionally spheroidal pyrite (light gray, almost white), galena (light gray) locally in delicate, rhythmic to concentrically layered alternations, and numerous small euhedral plates and crystal aggregates of barite (dark gray, almost black). At times galena, partly associated with covellite (dark gray), constitutes fine-grained interstitial fillings and cements narrow fractures and/or shrinkage cracks in schalenblende. The latter occupies interstices within the adjacent coarse crystal aggregate of barite and coats, partly as a thin "intergranular film", its large plates euhedrally developed after {001}. At one place schalenblende heals a fracture, while it is in turn thinly coated by galena. Gangue material, natural cavities and pores (all likewise dark gray, almost black).
Polished section, ×65.

Melnikovite-pyrite (Figs. 2, 12, 19) can be found as a major or minor ore component, usually associated with pyrite, marcasite, "intermediate product", and schalenblende. Melnikovite-pyrite is associated with other sulfides to constitute colloidal masses of rhythmically layered, botryoidal to reniform, and concentrically layered precipitates.

Marcasite (Fig. 19), although a possible major constituent in the present paragenesis, only constitutes a minor mineral component. It is found intergrown with pyrite, melnikovite-pyrite, "intermediate product", and schalenblende in colloidal masses and partially paramorphosed by pyrite.

"Intermediate product" (Figs. 2, 19) is found occasionally as a subordinate mineral constituent, usually in paragenesis with melnikovite-pyrite.

Chalcopyrite (Figs. 11, 20, 22, 24) is yet another minor mineral component, rarely constituting inclusions in sphalerite, schalenblende, or pyrite. In addition, chalcopyrite occurs as part of euhedral, heterogeneous aggregates (Figs. 20, 22) intergrown with fine-grained, partially euhedral pyrite, some galena, sphalerite, and enargite. Chalcopyrite may occupy a considerable part of these aggregates. Furthermore, enargite rims euhedral aggregates, filling fractures or shrinkage cracks, particularly in chalcopyrite. Additionally, chalcopyrite is encountered in extremely fine-grained masses in paragenesis with pyrite, galena, sphalerite, and enargite.

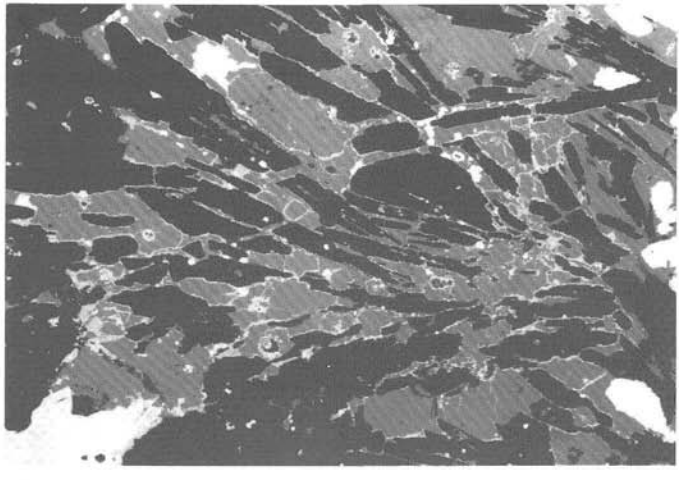

Fig. 11. Sample SO 41-181 FG 6.
Crystal aggregates of barite (dark gray, almost black) euhedrally developed after {001} are embedded in and, locally, somewhat replaced by sphalerite (medium gray). Sphalerite sporadically contains fine-grained pyrite (light gray, almost white) and galena (light gray) as well as tiny inclusions of chalcopyrite (likewise light gray) in places. Galena and covellite (dark gray) mostly occur within sphalerite as a delicate interstitial filling. The former two also cement fractures and/or shrinkage cracks in sphalerite and constitute a thin coating around it in contact to barite, even in places where sphalerite in turn cements cracks in barite. Fractures in sphalerite are in addition filled by enargite (light medium gray) and occasionally by chalcopyrite. Enargite is locally encountered in delicate myrmekitic intergrowth with pyrite (lower left corner, barely visible in photomicrograph). Polished section, ×130.

Enargite (Figs. 11, 20-25, 29) is a subordinate mineral constituent. It preferentially forms a part of heterogeneous, euhedral aggregates (Figs. 20-22, 24) composed mainly of either fine-grained, partially euhedral pyrite with minor interstitial enargite ("matrix" — Figs. 20-22, 24) or a mixture of chalcopyrite, fine-grained, partially euhedral pyrite, some sphalerite, galena, and enargite. Rims around these euhedral aggregates are constituted by sphalerite and enargite or, locally, by bravoite. Characteristic rims further emphasize the euhedral shape of "polysulfide" aggregates. Enargite is found finely intergrown with partly euhedral pyrite, chalcopyrite, galena, and sphalerite as well. It also occurs as rims and intergranular coatings around sphalerite and tabular barite, with healing cracks in the former. Locally, enargite fills shrinkage cracks, particularly in chalcopyrite.

In interstices of the above mentioned euhedral "polysulfide" aggregates, enargite is sporadically encountered in euhedral, squatly prismatic development, partially associated with euhedral galena and crystal aggregates of covellite (Fig. 24). A further peculiarity is the myrmekitic intergrowth of enargite and pyrite (Figs. 11, 25).

Wurtzite is extremely rare and appears only as fine-grained crystals developed after {0001} in the center of schalenblende aggregates.

Covellite (Figs. 10-11, 22, 24) is an accessory mineral often forming small, occasionally euhedral aggregates. Besides ordinary covellite its **"permanent blue" variety** is present. The mineral is often found associated with galena as a cavity lining in or interstitial to sphalerite and schalenblende. In addition, covellite and galena constitute rims and intergranular coat-

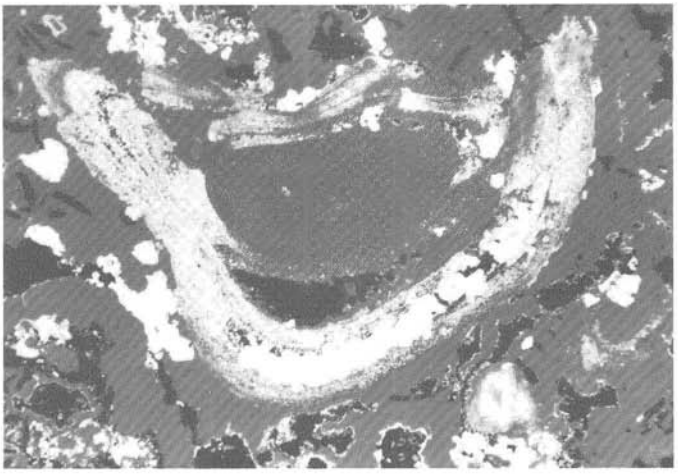

Fig. 12. Sample SO 41-181 FG 6.
Schalenblende (dark medium gray) reveals zones of rhythmically layered alternations mainly with galena (light gray), which clearly show distortion, and even folding (slump folding, slumping). Additionally, schalenblende contains occasional barite plates (black) after {001} and pyrite (light gray, almost white). The latter occurs in cavities and, partly in the presence of melnikovite-pyrite (light gray to medium gray), in spheroids which are associated with galena in the alternations. In cavities and interstices of schalenblende accretions and coatings, as well as tiny crystals of galena, can be seen. Gangue material, natural cavities and pores (all likewise black).
Polished section, oil immersion, ×85.

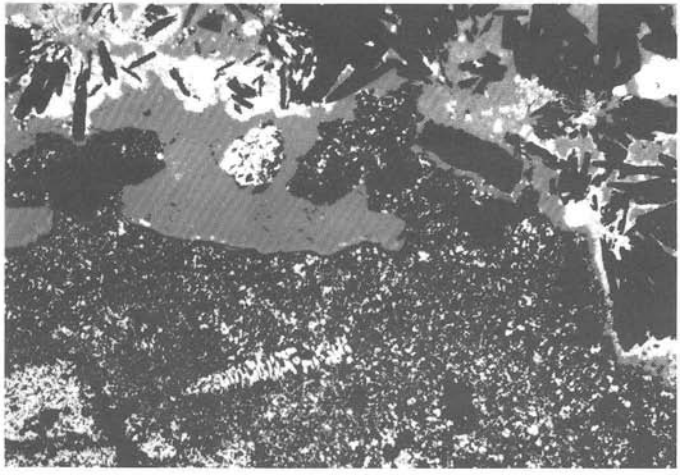

Fig. 13. Sample SO 41-181 FG 9.
In places, Schalenblende (dark gray) shows rhythmically layered alternations with galena (light gray) and contains abundant crystal aggregates of barite (black), which in turn are rimmed by galena. Along its periphery, schalenblende is surrounded by fine-grained, porous galena occasionally exhibiting dendritic aggregates and crystal skeletons. Sporadic occurrences of pyrite (light gray, almost white), partly spheroidal, accompanied by galena, are encountered in schalenblende. Gangue material, natural cavities and pores (all likewise black).
Polished section, oil immersion, ×165.

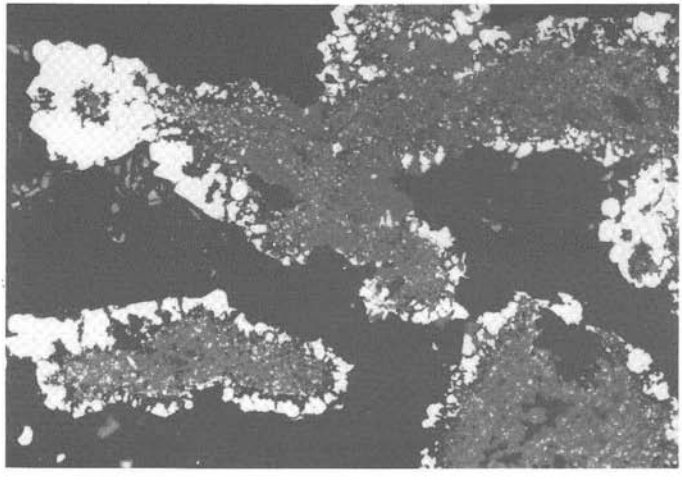

Fig. 14. Sample SO 41-181 FG 9.
Dendritic schalenblende (dark gray) containing abundant inclusions of fine-grained galena (light gray) and a small amount of pyrite (light gray, almost white) reveals peripheral accretion and/or coating of coarser grained, partly euhedral galena (depositional fabrics). The latter is itself rimmed by pyrite and its typical spheroids. Gangue material, natural cavities and pores (all black).
Polished section, oil immersion, ×165.

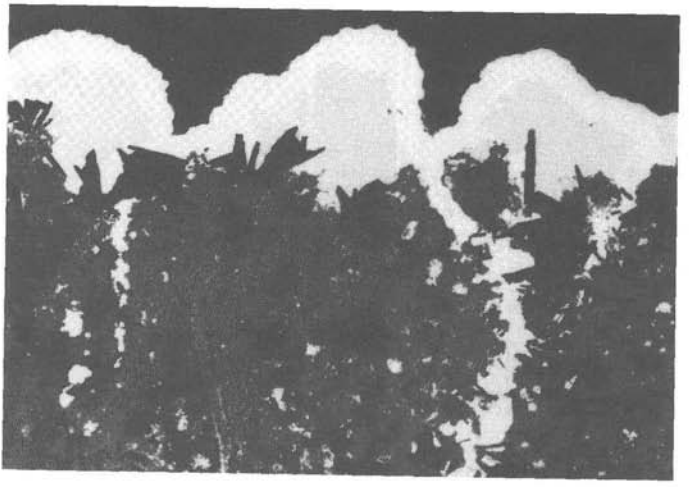

Fig. 15. Sample SO 41-181 FG 9.
Dendritic schalenblende (dark gray) contains frequent inclusions of tabular barite crystals (black) and fine-grained galena (light gray), which is also present in larger crystal aggregates around the margins of schalenblende. All of these are rimmed by pyrite (brighter light gray), additionally filling fractures in schalenblende. Natural cavities and pores (all likewise black).
Polished section, oil immersion, ×85.

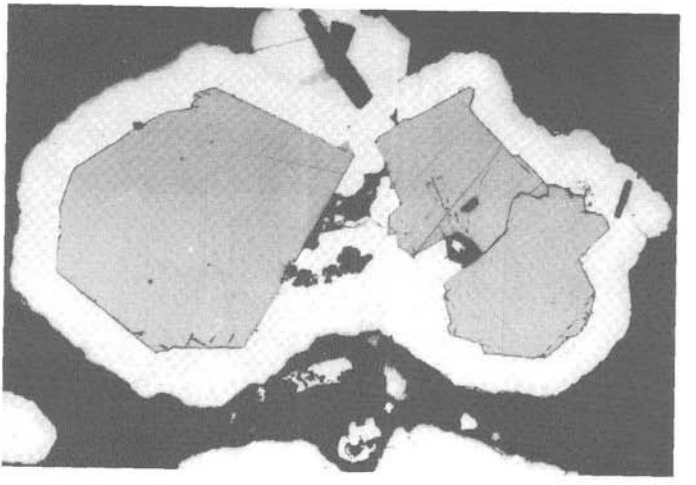

Fig. 16. Sample SO 41-181 FG 9.
Crystal aggregates of galena (medium gray) are completely rimmed by pyrite (light gray, almost white), which in turn is overgrown by an extremely thin coating of bravoite (light gray). Locally, pyrite embraces tiny inclusions of schalenblende (black) and euhedral plates of barite (likewise black). Furthermore a tiny plate of the latter is contained in galena. One pyrite spheroid can be seen. Natural cavities and pores (all likewise black).
Polished section, oil immersion, ×135.

ings around sphalerite and barite, also filling shrinkage cracks in them. Covellite is also found in intimate intergrowths with galena, chalcopyrite, enargite, sphalerite, and partially euhedral pyrite, as well as in mixtures of these minerals, forming euhedral "polysulfide" aggregates. Interstices in the latter rimmed by bravoite locally show overgrowth of covellite.

Bravoite (Figs. 16, 26-28) is another accessory constituent. It appears locally as fine rims around pyrite, either filling cavities and interstices, e. g. in and around sphalerite and schalenblende, or enclosing euhedral galena. Bravoite, in turn, may be overgrown by pyrite. The changing habit of euhedral bravoite aggregates as their growth continued, is locally observed as the typical zoning of bravoite. Rhythmic concentric to conchoidal spheroids and thin, rhythmically layered to conchoidal accretions (Fig. 27) of bravoite are observed sporadically. Furthermore, bravoite sparsely rims euhedral aggregates composed of fine-grained, partly euhedral pyrite and other sulfides which are otherwise rimmed by enargite and sphalerite. Additionally, bravoite constitutes rims along cavities and interstices within the complex, euhedral "polysulfide" aggregates, also revealing overgrowth by covellite and galena itself.

Tennantite (Figs. 24, 29-32) is an accessory mineral encountered, usually in association with enargite, in rims and interstices of euhedral "polysulfide" aggregates. Tennantite is also intergrown with galena and chalcopyrite.

A lead sulfosalt, probably **jordanite** (Fig. 33), represents a true curiosity. It was identified in the center of concentrically layered schalenblende, as well as in radial inclusions

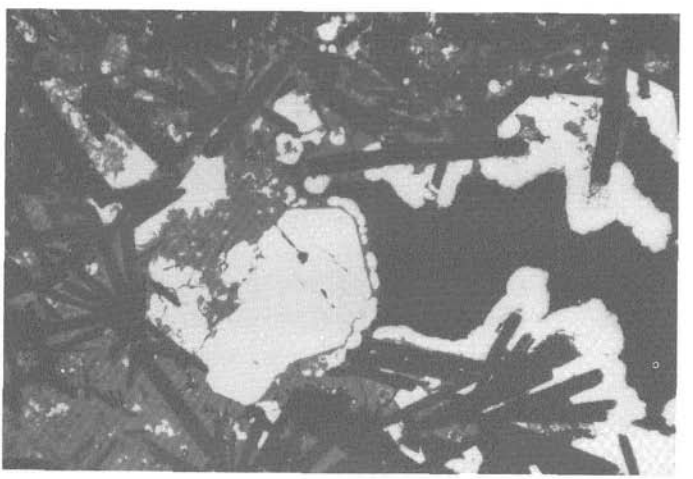

Fig. 17. Sample SO 41 -181 FG 9.
Schalenblende (dark gray) comprises abundant inclusions of barite crystal aggregates (black) along with small amounts of galena (light gray) and pyrite (light gray, almost white), which locally forms spheroids. Schalenblende completely fills the interstices within crystal aggregates of barite. Overgrowth of galena produced a larger euhedral aggregate which is peripherally, very thinly in places, coated by schalenblende, which is itself in turn rimmed by pyrite (light gray, almost white). The latter also exhibits rims around euhedral barite plates or their thin schalenblende coatings ("films") and furthermore occupies interstices among the barite crystal aggregates. Natural cavities and pores (both likewise black).
Polished section, oil immersion, ×65.

associated with galena enclosed in the zinc sulfide. The presence of jordanite is evidenced by its high reflectivity (trace lower than galena), its color, its weak bireflection, and its anisotropism.

Limonite is occasionally encountered. Its presence indicates that submarine weathering (halmyrolysis) and oxidation have already commenced.

2.2. Gangue material

The amount of gangue material in the present complex massive sulfide specimens varies considerably. **Barite,** the major gangue material (Figs. 2-3, 6-7, 9-13, 15-17, 19, 31-32, 35, 38), usually forms tabular crystals developed after {001}. The crystals are of varying size, even when in close spatial association with each other, and may locally dominate or be completely subordinate. Consequently, barite plates and crystal aggregates occur frequently in large amounts, often engulfed by ore minerals. Their interstices display excellent fillings of mainly schalenblende, sphalerite, pyrite, and melnikovite-pyrite. In other places only sparse barite plates and platelets are enclosed in sulfide minerals. Accretions and overgrowths of sulfides such as schalenblende, galena, and pyrite on and around barite plates are widespread. The same applies to thin rims and intergranular coatings, for example of schalenblende, galena, and/or covellite. Ore mineral inclusions in euhedral barite are rarely encountered, while occasional fractures and cracks are filled with sulfides (e. g. schalenblende).

The typical bubble-like spheroids displaying a superficial shell of pyrite often contain a center of barite, which in many cases exhibits crystal aggregates. Shrinkage cracks are com-

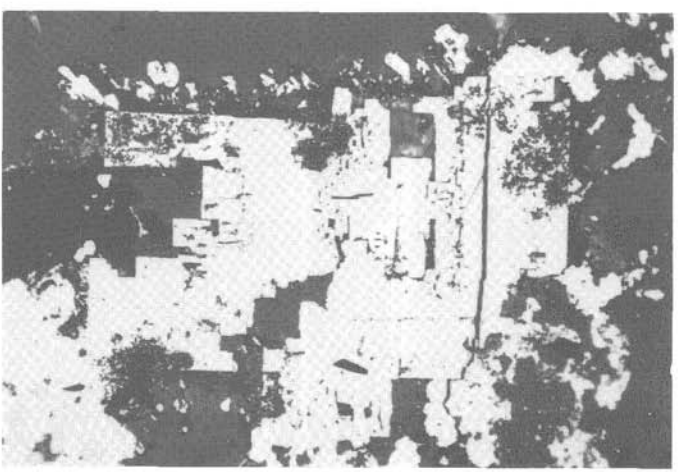

Fig. 18. Sample SO 41-181 FG 6.
Skeleton crystal aggregate of galena (light gray, almost white) developed after {100} in places exhibits delicate myrmekitic intergrowth with gangue material (black). Both are embedded in schalenblende (dark gray, internal reflections), accompanied by pyrite (likewise light gray, almost white) and a small amount of galena. Schalenblende constitutes fillings of interstices in the euhedral galena aggregate. Both exhibit peripheral overgrowth of fine-grained, partly dendritic to skeletal galena. Natural cavities and pores (both likewise black).
Polished section, oil immersion, ×275.

mon in the baryte occupying the center. These shrinkage cracks can be cemented by galena and pyrite.

2.3. Microorganisms within the complex massive sulfide ores

In some of the complex massive sulfide ore specimens, microorganisms are contained and preserved, namely replaced and pseudomorphed by above all zinc sulfide (sphalerite, schalenblende) and some pyrite (Figs. 34-37). The materials examined constitute microbial mats, probably laminated bacterial mats from sheath-forming cyanobacteria or colorless sulfur bacteria. In polished sections, central parts of these laminated bacterial mats are cross cut, revealing fossilized bacterial sheaths and/or bacterial cell walls, while the peripheral or outer parts showing longitudinal sections. It can therefore be concluded that origininally hemispherical bodies of these bacterial mats were present. Irregular and annual ring-like structures indicate fluctuating growth conditions, presumably caused by changes in the environmental factors, such as temperature and sulfide concentration.

Neither knots, cross linkages nor nets could be observed, which excludes the presence of both fungi and sulfur bacteria. The cutting positions seen in the polished sections disclose some similarities with cross sections of Cnidaria (e. g. *Lithophyllum, Chaetes,* Anthozoa, Tabulata, or *Milleporidium,* Hydrozoa, Strommatoporoidea). However, because of the substantially smaller dimensions of the laminated microbial mats a classification to Cnidaria is also excluded.

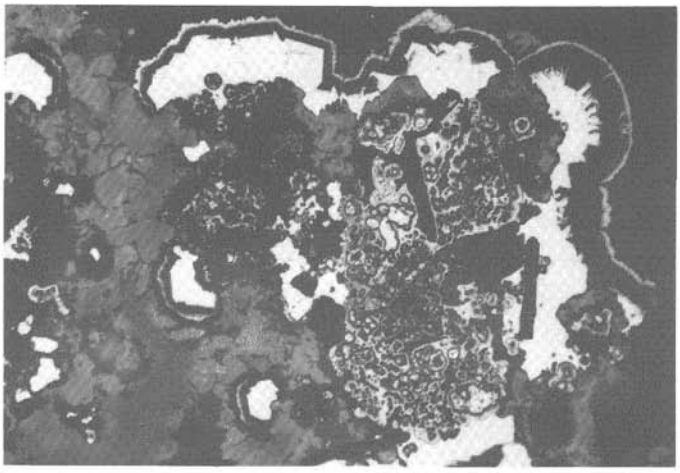

Fig. 19. Sample SO 41 -181 FG 7.
Colloidal masses of schalenblende (dark gray in different shades because of internal reflections) and rhythmically layered, mostly concentric melnikovite-pyrite (medium gray to dark gray) associated with some "intermediate product" (medium gray to dark gray, almost black), display the accretion of pyrite (light gray, almost white) and euhedral marcasite (likewise light gray, almost white), partly paramorphed by pyrite, followed by "intermediate product" and melnikovite-pyrite in cavities and around their edges. Occasional barite plates (black) occur. Natural cavities and pores (all likewise black).
Polished section, oil immersion, ×275.

3. Conclusions and Future Prospects

The present ore specimens from the sediment of the Palinuro Seamount represent a complex paragenesis of sulfides, sulfosalts, and sulfate gangue material. Major constituents of the mineral paragenesis are pyrite, melnikovite-pyrite, sphalerite, schalenblende, galena, and barite, while chalcopyrite and enargite are minor constituents. The presence of enargite and tennantite gives evidence for the occurrence of an iron-poor base metal mineralization.

Mineral phases are usually intimately intergrown, often rich in inclusions, and composed to a considerable extent of complex sequences to rhythmic alternations mostly of schalenblende, melnikovite-pyrite, pyrite, and galena, but not of chalcopyrite and enargite.

Widespread, excellent, colloform, colloidal and/or gel textures are a characteristic paragenetic feature for this type of mineralization. These types of ore intergrowths are generally attributed to low formation temperatures (e. g. P. RAMDOHR, 1975, 1981).

Textural evidence, such as (syn-) sedimentary deformation, indicates that the original ore mud underwent distortion in an unconsolidated state. This is documented by plastic deformation (slump folding, slumping) of rhythmic layers and alternations, mainly of galena, contained in and associated with sphalerite and schalenblende.

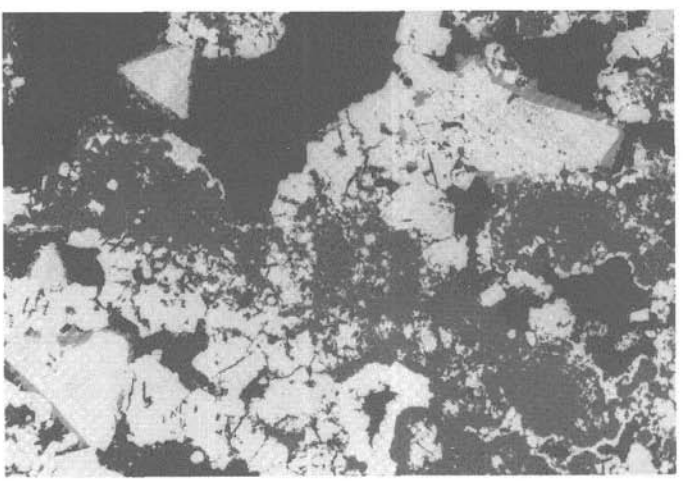

Fig. 20. Sample SO 41-181 FG 10.
Dendritic aggregates of schalenblende and sphalerite (both dark gray), in places rimmed by some pyrite (light gray, almost white, e. g. below center and lower left corner of photomicrograph) and overgrown by a euhedrally outlined aggregate (upper right half of photomicrograph), but predominantly by galena (light gray, in photomicrograph hardly distinguishable from pyrite), exhibiting crystal aggregates. Besides the one euhedral aggregate overgrowing schalenblende, two more can be observed (lower and upper left half of photomicrograph), all three of them consisting mainly of fine-grained, partly euhedral pyrite and small amounts of sphalerite, chalkopyrite (likewise light gray) and enargite (medium gray). These euhedral aggregates are rimmed by enargite and are also overgrown by and embedded in fine-grained, porous galena crystal aggregates. The latter can be observed with traces of chalcopyrite as inclusions within the schalenblende dendrites. Gangue material (black).
Polished section, oil immersion, ×100.

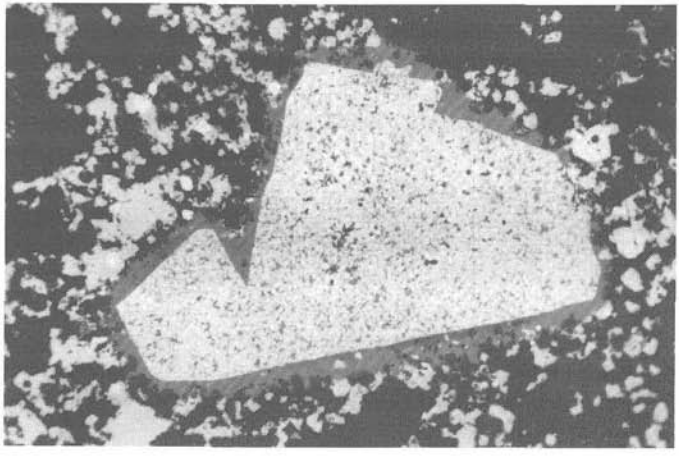

Fig. 21. Sample SO 41 -181 FG 9.
Enargite (medium gray) encloses and rims a heterogeneous, euhedral aggregate composed almost entirely of fine-grained, partly euhedral pyrite (light gray, almost white) and a small amount of interstitial enargite ("matrix"). The frequently occurring galena (light gray) is encountered in small, partly euhedral aggregates accompanied by schalenblende (dark gray, almost black) and small amounts of pyrite, forming spheroids in places. Gangue material, natural cavities and pores (all black).
Polished section, oil immersion, ×425.

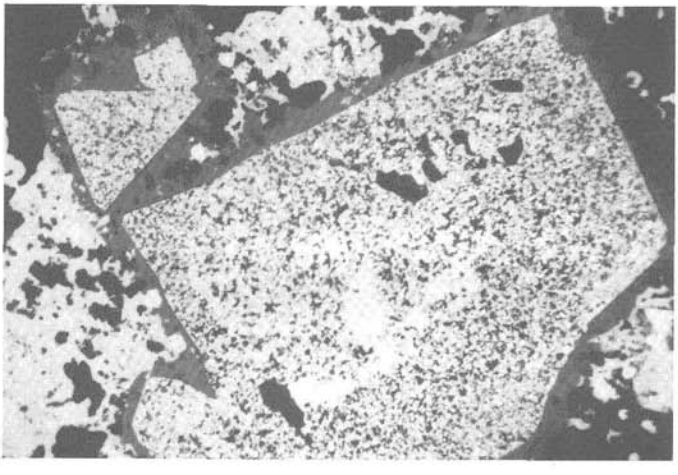

Fig. 22. Sample SO 41 -181 FG 6.
Larger euhedral aggregates are chiefly composed of chalcopyrite (light gray) and fine-grained, partly euhedral pyrite (light gray, almost white), and interstitially filled ("matrix", barely discernible in photomicrograph) by covellite (dark gray, almost black), enargite (dark medium-gray) and sphalerite (likewise dark gray, almost black). The euhedral shape of the larger, heterogeneous aggregates are strikingly emphasized by an enargite rim. In contrast to this, pyrite is also found locally in rhythmically layered to concentric masses, in association with schalenblende and some galena (likewise light gray). Gangue material, natural cavities and pores (all black).
Polished section, oil immersion, ×425.

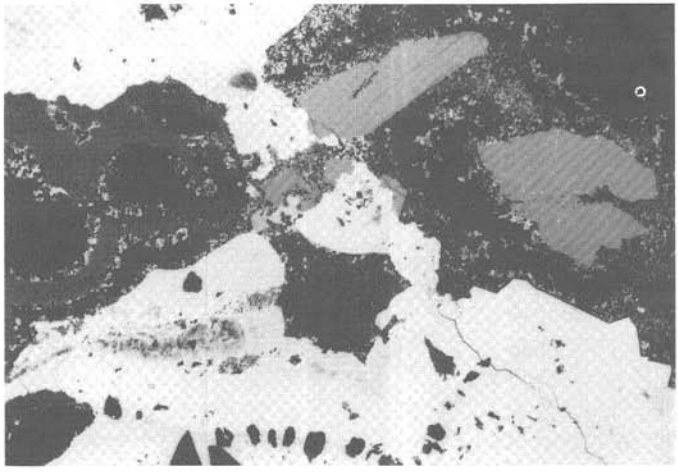

Fig. 23. Sample SO 41-181 FG 10.
Aggregates of pyrite (different shades of light gray, almost white), partly euhedral and partly exhibiting zonal arrangements with small amounts of fine-grained galena (light gray). Pyrite is overgrown by enargite (medium gray) and bubble-like spheroids of schalenblende (dark gray), all of these in turn overgrown and partly rimmed by fine-grained, porous crystal aggregates of galena. Gangue material, natural cavities and pores (black).
Polished section, oil immersion, ×130.

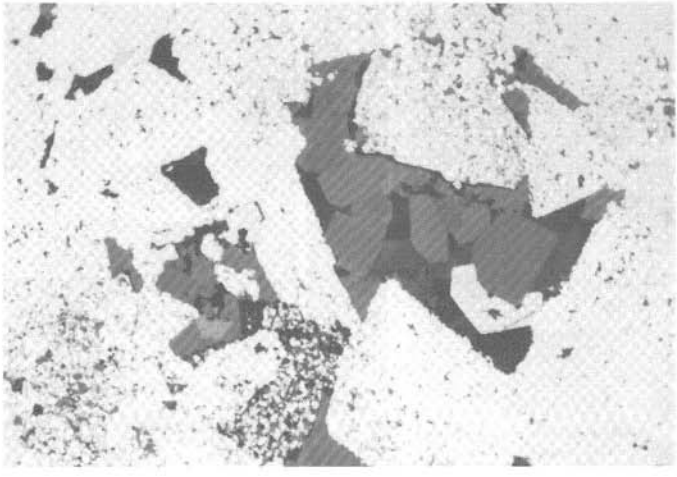

Fig. 24. Sample SO 41-181 FG 6.
Euhedral enargite (medium gray in different shades because of bireflection), crystal aggregates of covellite (dark gray to almost black, bireflection), some galena (light gray) partly exhibiting euhedral shape, and a trace of tennantite (light medium-gray) constitute interstices and/or cavity fillings between heterogeneous, euhedral aggregates. The latter are composed of partly euhedral pyrite containing interstitial enargite ("matrix") or of pyrite embedded in chalcopyrite (likewise light gray), enargite, and locally galena and sphalerite (dark gray, almost black).
Polished section, oil immersion, ×1075.

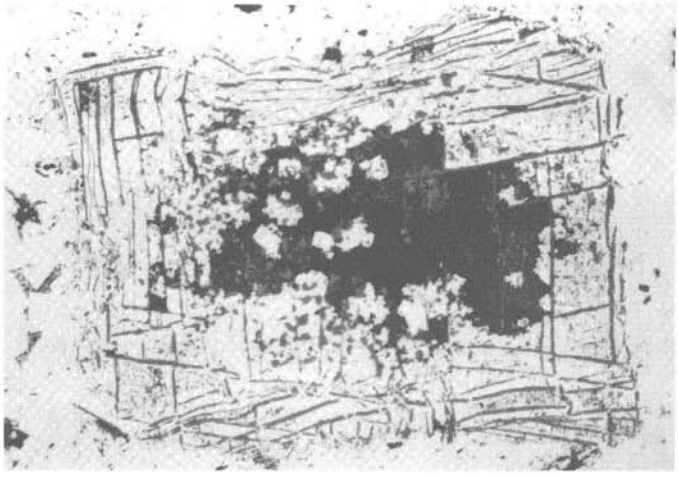

Fig. 25. Sample SO 41-181 FG 7.
Delicate myrmekite of pyrite (light gray) with enargite (dark gray) around a central cavity. Some gangue material (almost black, in places brightened by internal reflections).
Polished section, oil immersion, ×425.

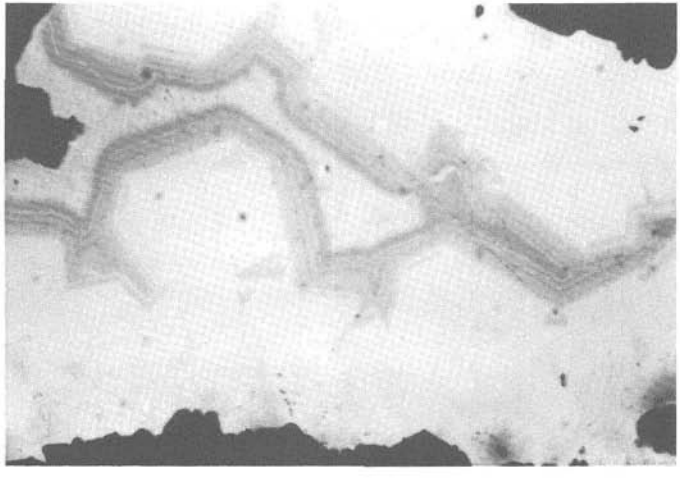

Fig. 26. Sample SO 41-181 FG 9.
Euhedral pyrite (light gray) is rimmed by bravoite (medium gray in different shades) which exhibits distinctive zoning and is itself in turn overgrown by ordinary pyrite. Peripheral schalenblende (black) occur.
Polished sections, oil immersion, ×1075.

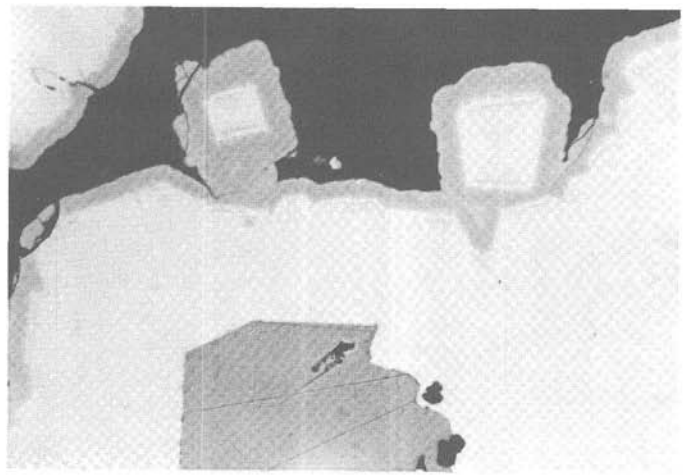

Fig. 27a.

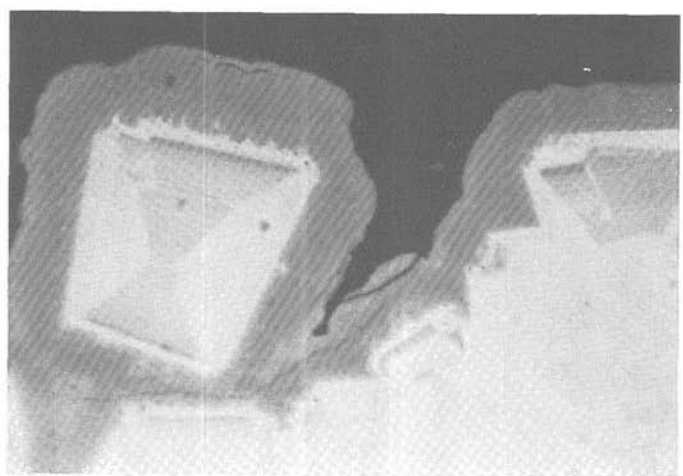

Fig. 27b.

Fig. 27. Sample SO 41-181 FG 9.
Euhedral galena (dark medium gray) is enclosed in pyrite exhibiting euhedral shapes, which in turn is coated by bravoite (medium gray in different shades). The latter shows distinctive zoning and rhythmically layered accretions along its margins. Schalenblende (black) is locally embedded in galena and pyrite or growing peripheral to bravoite.
Polished section, oil immersion, Fig. 27a: ×425,
Fig. 27b (Detail of Fig. 27a): ×1075.

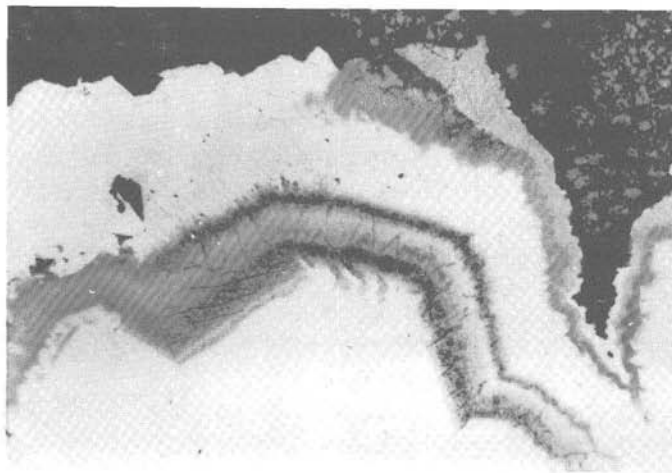

Fig. 28. Sample SO 41-181 FG 10.
Crystal aggregates of pyrite (light gray), exhibiting distinct rhythmic zonal arrangements with bravoite (light medium-gray) and galena (dark medium-gray) and some gangue material (black). In zones of the latter three minerals shrinkage cracks can be observed and in places fillings with fine-grained, porous crystal aggregates of galena, which can also be seen outside the pyrite crystal aggregate.
Polished section, oil immersion, ×400.

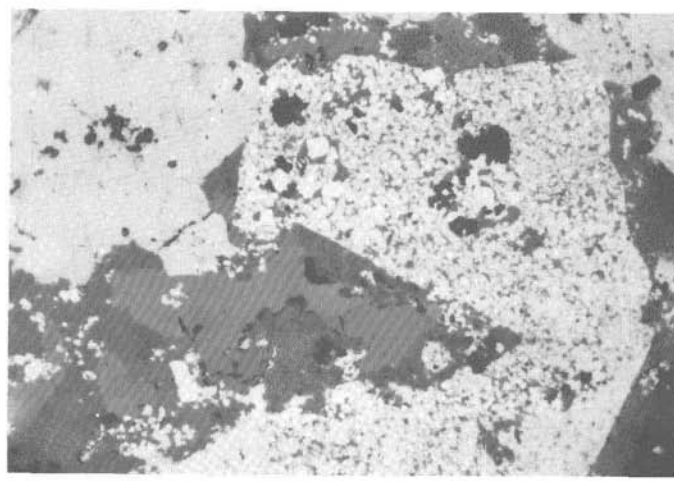

Fig. 29. Sample SO 41-181 FG 6.
Tennantite (medium gray) intergrown with enargite (dark medium gray) and galena (light gray), all of which constitute a rim around a heterogeneous, euhedral aggregate. The latter is preponderantly composed of fine-grained, partly euhedral pyrite (light gray, almost white) and minor sphalerite (almost black), which are embedded in an enargite matrix. Some gangue material (black).
Polished section, oil immersion, ×1075.

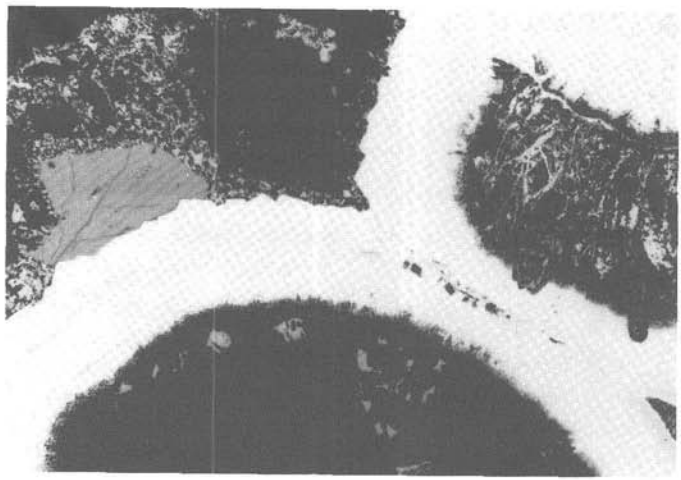

Fig. 30. Sample SO 41-181 FG 10.
Crystal aggregate of tennantite (medium gray) grown on pyrite (light gray, almost white), forming the superficial shell of bubble-like spheroids. Tennatite and pyrite are overgrown by fine-grained, porous crystal aggregates of galena (light gray). The center of the bubble-like spheroids is composed of gangue material (black), containing pyrite and galena as inclusions, mostly as healings and fillings of fractures and shrinkage cracks.
Polished section, oil immersion, ×160.

Fig. 31. Sample SO 41-181 FG 10.
Euhedral plates of barite (black) rimmed by fine-grained, porous crystal aggregates of galena (light gray), which also fills interstices within the barite crystal aggregates. Within its masses of mostly fine-grained, porous crystal aggregates of the galena euhedral pyrite (light gray, almost white) and euhedral tennantite (medium gray) can be observed, both of which are rimmed by the galena crystal aggregates. Gangue material, natural cavities and pores (all likewise black).
Polished section, oil immersion, ×130.

Shrinkage cracks preponderantly filled with galena or pyrite, locally accompanied by covellite or occasionally by enargite, are observed in places. Diagenetic processes are also considered to account for the appearance of galena as characteristic overgrowths, accretions, and cavity fillings.

It is worth mentioning that the diagenetic textures found in the Palinuro Seamount mineralization are, in terms of carbonate sedimentology, not only diagenetic textures but even late diagenetic textures. This becomes clearly evident on comparison with similar and even identical textures within carbonate hosted base metal deposits (e. g. especially Bleiberg-Kreuth/Carinthia and Mežica-Topla/Slovenia type localities).

The variety of the mineral paragenesis and its complex intergrowths exemplify the complex chemical composition, including major elemental constituents as well as trace elements, along the lines with the precious metal content of this base metal mineralization.

A further particular charactersitic constitutes proof for the existence of microorganisms, namely the observation of microbial mats, most of these presumably laminated bacterial mats, preserved and pseudomorphed by sphalerite, schalenblende and some pyrite in this complex massive sulfide mineralization. This observation documents an excellent example of modern fossilization. Furthermore, this wholly unexpected and exciting result discloses essential information about the microbial communities associated with the hydrothermal springs which have formed the Palinuro Seamount complex massive sulfide mineralization.

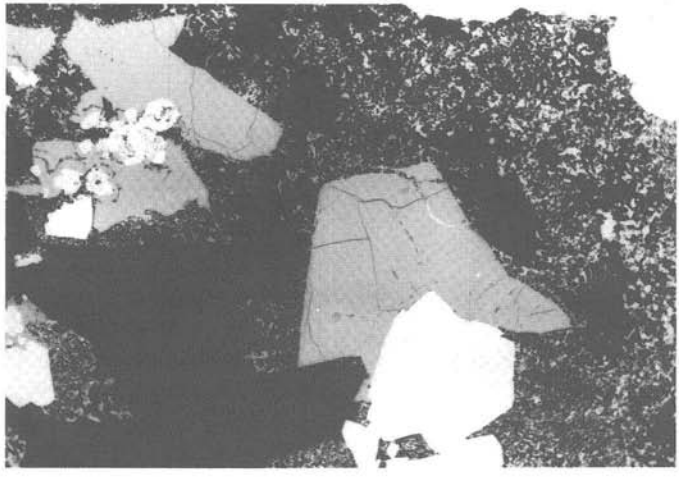

Fig. 32. Sample SO 41-181 FG 10.
Euhedral plates of barite (black), in places overgrown by crystal aggregates of tennantite (medium gray) and pyrite (light gray, almost white), all embedded within masses of fine-grained, porous crystal aggregates of galena (light gray), which also rims the other minerals. The euhedral tennantite shows fractures revealing even a faint cleavage with a few fractures cemented by pyrite and fine-grained crystal aggregates of galena (right of center of photomicrograph). Locally, the tennantite fills interstices around pyrite crystal aggregates. In places, tennantite exhibits rhythmically layered textures with schalenblende (dark gray, almost black), which also can be found in similar delicate colloform textures intergrown with partly euhedral aggregates of pyrite within the tennantite (lower left half of photomicrograph).
Polished section, oil immersion, ×130.

In this context it is also worth mentioning that microorganisms and particularly microbial mats have only been recognized since a few years ago as a typical and important part of vent communities associated with hydrothermal vents (e. g. S. BELKIN and H. W. JANNASCH, 1989, Y. COHEN and E. ROSENBERG, 1989, H. W. JANNASCH and C. O. WIRSEN, 1981, D. M. WARD et al., 1989).

A comparison of the complex Palinuro Seamount ores with modern black smoker material from active divergent plate margins of the Pacific (East Pacific Rise, Galápagos Rift — W. TUFAR, 1987, 1988, 1989, 1990, 1991, W. TUFAR et al., 1984, 1985, 1986 a, 1986 b, 1987) at first seems reasonable, but both types show only few common characteristics. Similarities in paragenesis are partly revealed by the major sulfide components (pyrite, melnikovite-pyrite, sphalerite, schalenblende) and their typical intergrowths (colloidal and/or gel textures), as well as a high porosity, common to both types of complex massive sulfide ore.

However, some differences concerning paragenetic association of ore minerals are evident. Black smokers from the East Pacific Rise are characterized by the occurrence of high-temperature sulfides (chalcopyrrhotite, high-temperature chalcopyrite), which were not observed in the present Palinuro Seamount samples. There, chalcopyrite is only a minor component, while it represents a major constituent of complex massive sulfide ores from the East Pacific Rise or the Galápagos-Rift. Accordingly, galena and enargite are typical

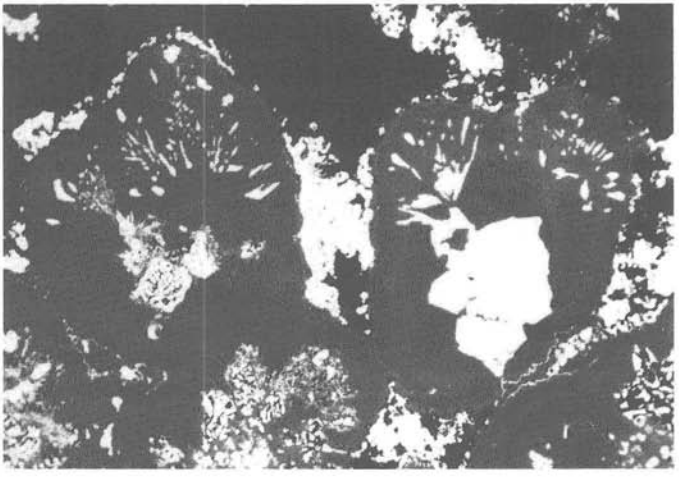

Fig. 33. Sample SO 41-181 FG 6.
Rhythmic, concentrically layered schalenblende (dark gray in different shades — the slight variations in its reflectivity denote zoning) contains partly skeleton crystals of galena (light gray, almost white) in the center. In one aggregate of schalenblende (right half of photomicrograph) there is a small amount of galena adjacent to a lead sulfosalt, probably jordanite (slightly lower reflectivity than galena, in photomicrograph hardly distinguishable from galena), which locally exhibits radial inclusions in the peripheral parts of schalenblende (upper half of photomicrograph). Pyrite (almost white) overgrows schalenblende, also constituting interstitial fillings within its aggregates. Locally, the periphery of schalenblende shows delicate rhythmically layered alternations with galena. Gangue material, natural cavities and pores (all black).
Polished section, oil immersion, ×275.

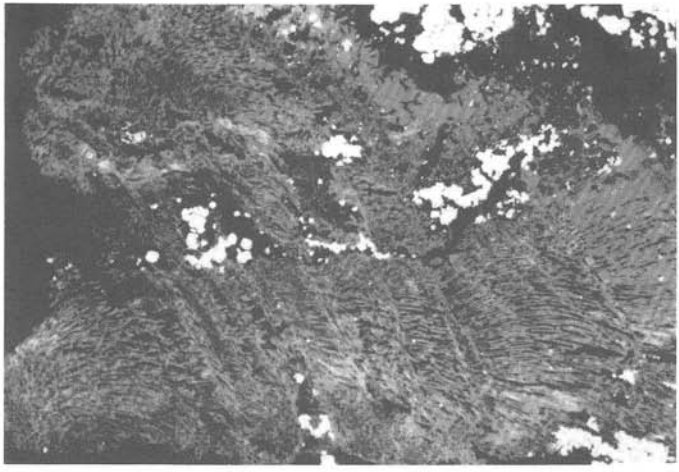

Fig. 34. Sample SO 41-181 FG 10.
Microbial mats, presumably bacterial mats, replaced and pseudomorphed by sphalerite and schalenblende (both dark gray), exhibiting the center of a hemispherical bacterial mat with annual ring-like structures. In places, peripherally some pyrite (light gray, almost white) can be observed. Gangue material, natural cavities and pores (all black). Polished section, oil immersion, ×15.

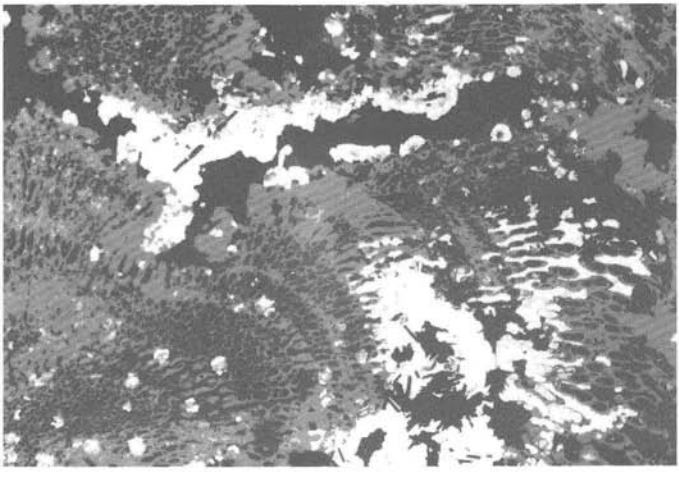

Fig. 35. Sample SO 41-181 FG 10.
Sphalerite (dark gray), pseudomorphous after a microbial mat, presumably a bacterial mat, revealing clearly cross cut microbial, i. e. bacterial filaments. In places, pyrite (light gray, almost white) replaces sphalerite, which is also rimmed by pyrite. Within the pyrite inclusions, barite crystal aggregates (black) can be observed (right lower half of photomicrograph). Gangue material, natural cavities and pores (all likewise black).
Polished section, ×35.

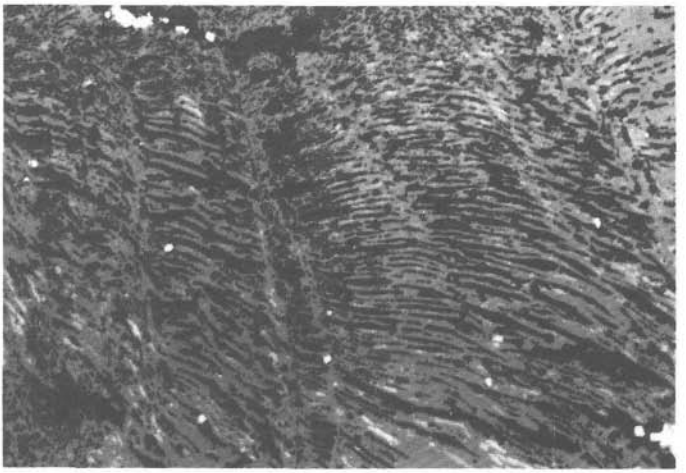

Fig. 36. Sample SO 41-181 FG 10.
Microbial mat, presumably bacterial, replaced and pseudomorphed by sphalerite (dark gray), disclosing cross cut as well longitudinally cut sections of a hemispherical bacterial mat and its mostly longitudinally cut filaments. Locally, small amounts of pyrite (light gray, almost white) can be seen. Gangue material, natural cavities and pores (all black). Polished section, ×35.

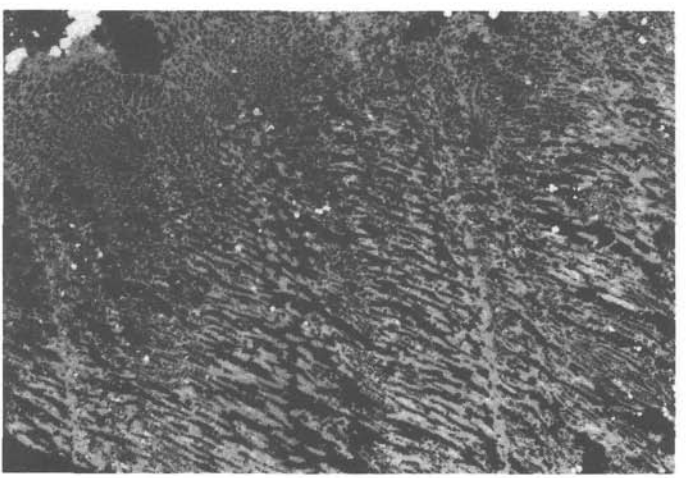

Fig. 37. Sample SO 41-181 FG 10.
Sphalerite pseudomorph (dark gray), exhibiting mostly longitudinal section of a microbial mat, presumably bacterial, and its longitudinally cut filaments, as well as annual ring-like structures. Locally, small amounts of pyrite (light gray, almost white) can be observed. Gangue material, natural cavities and pores (all black).
Polished section, ×35.

Palinuro Seamount sulfides, the former as a major, the latter as a minor constituent. In contrast, galena is a mere accessory mineral, while enargite is completely absent in specimens from the East Pacific Rise.

Furthermore, considerable differences are exemplified by the nature of the gangue material. While X-ray amorphous silica (opaline silica) is locally abundant even in samples from the East Pacific Rise and the Galápagos Rift, it was not identified in Palinuro Seamount complex massive sulfide samples containing barite as a major mineral constituent.

In addition, one can attempt to compare the Palinuro Seamount occurrence with the recently discovered complex massive sulfide mineralizations from the Manus Spreading Center in the Bismarck Sea (W. TUFAR, 1990 b). These mineralizations are, for example, distinguished by black smoker chimneys mostly rich in zinc, in places by substantial contents of barite and galena and occasionally extremely high traces of gold (1.3-52.5 ppm Au) and substantial traces of silver (25-1036 ppm). Concerning, for example enargite, the Manus Spreading Center mineralizations are also characterized by a lack of this particular mineral.

Massive sulfide specimens from the Kebrit Deep of the Red Sea (Station SO 29 — Dredge 354) exhibit an ore paragenesis of only three sulfides (pyrite, schalenblende and galena), distinctly displaying the effects of diagenesis. Noteworthy are inclusions of microorganisms (foraminiferid tests, diatom frustules) in the Red Sea massive sulfides. A comparison of mineral parageneses of complex massive sulfide ores from the Palinuro Seamount, modern black smokers from the East Pacific Rise, Galápagos Rift, and Manus Spreading Center (Bismarck Sea/Papua New Guinea) and massive sulfide ores from the Kebrit Deep of the Red Sea reveals certain similarities, but also significant genetic differences.

Fossil syngenetic base metal deposits are comparable to complex massive sulfide ores from the Palinuro Seamount in the Tyrrhenian Sea in terms of mineral intergrowths, textures, sedimentary deformation, and diagenesis, and are thus suitable for comparison. Examples are constituted by the ore deposits of e. g. Rammelsberg (Harz/Germany), Meggen/Lenne (Sauerland/Germany), lead-zinc ore deposits of the Eastern Alps, such as Bleiberg-Kreuth (Carinthia/Austria) and Mežica-Topla (Slovenia), a recently discovered Palaeozoic lead-zinc deposit in Nevada/USA (W. Tufar et al. 1984), and Veovača (Bosnia).

Concerning the textures occurring, as well as the paragenesis, one can — with some caution — attempt to make comparisons with the Veovača deposit in Bosnia (Figs. 38-39).

This syngenetic base metal deposit is, for example, comparable to the Palinuro Seamount mineralization, also characterized by galena and barite as major mineral constituents. Furthermore, mercury is found in substantial traces in the Veovača base metal paragenesis, as well.

Even though there are some possibilities for drawing comparisons with other modern finds, as well as with ancient ("fossil") base metal deposits, it can be asserted from the paragenetic point of view that the Palinuro Seamount complex massive sulfide mineralization is somewhat unique.

Acknowledgements

I appreciate the support of Prof. Dr. H. Puchelt (Universität Karlsruhe) in providing samples. My thanks are also due to Dr. U. Siewers (Bundesanstalt für Geowissenschaften und Rohstoffe, Hannover) for his valuable assistance, as well as to Mr. L. A. Beck, Prof. Dr. W. Wehrmeyer (both Philipps-Universität Marburg), Dr. G. Gerdes (Meeresstation der

Fig. 38. Sample SO 41-181 FG 8 b.
Pyrite (light gray, almost white), containing numerous inclusions of euhedral tabular barite platelets (black) of different size and schalenblende (dark gray) along with small amounts of galena (light gray). In places, the schalenblende also constitutes spheroids (upper right corner of photomicrograph).
Polished section, ×65.

Fig. 39. Veovača (Bosnia).
Colloform, rhythmic, botryoidal-reniform, in parts concentric masses of pyrite (light gray, almost white), containing numerous inclusions of euhedral tabular barite (black) and spheroidal pyrite, as well as gangue material spheroids, together with a few schalenblende spheroids (dark gray). Locally, barite is replaced by schalenblende which also fills interstices within pyrite.
Polished section, ×65.

Universität Oldenburg, Wilhelmshaven) and Dipl.-Geograph Theo Topel (Georg Westermann Verlag, Braunschweig) for their valuable discussions. The critical review of the English manuscript by Dr. J. McMinn (Siemens AG, Erlangen) and Dr. W. Baum (Pittsburgh Mineral & Environmental Technology, Inc., New Brighton, Pennsylvania) is kindly appreciated.

4. References

BELKIN, S. and H. W. Jannasch: Microbial Mats at Deep-Sea Hydrothermal Vents: New Observations. — In: COHEN, Y. and E. ROSENBERG (Editors): Microbial Mats — Physiological Ecology of Benthic Microbial Communities, 16-21, Washington (D. C.) 1989.

COHEN, Y. and E. ROSENBERG (Editors): Microbial Mats — Physiological Ecology of Benthic Microbial Communities. — Washington (D. C.) 1989.

JANNASCH, H. W. and C. O. WIRSEN: Morphological Survey of Microbial Mats Near Deep-Sea Thermal Vents. — Applied and Environmental Microbiology, **41**, No. 2, 528-538, 1981.

Table 1. Chemical composition of hydrothermal complex massive sulfide ore samples (SO 41-181 FG) from the Palinuro Seamount

	5/1	5/2	6/1	6/2	8	9	10/1
				percent			
CuO	0.31	0.32	0.62	0.62	0.91	0.02	0.51
PbO	4.95	4.84	14.12	13.91	21.81	0.04	6.65
ZnO	20.35	21.06	16.85	17.30	28.15	0.12	14.61
SiO_2	0.17	0.23	0.13	0.18	0.10	0.55	0.32
TiO_2	0.01	0.01	0.03	0.03	0.01	0.01	0.01
Al_2O_3	0.41	0.33	0.59	0.38	0.39	0.19	0.43
Fe_2O_3*	28.51	27.97	15.18	15.17	14.28	57.57	31.94
MnO	0.02	0.02	0.02	0.03	0.02	0.06	0.02
CaO	0.02	0.02	0.02	0.03	0.06	0.59	0.04
Na_2O	0.52	0.61	0.47	—	—	1.84	2.41
K_2O	0.07	0.07	0.05	0.05	0.07	0.10	0.09
P_2O_5	0.02	0.01	0.02	0.01	—	0.03	0.01
SO_3	8.50	8.40	15.79	15.59	10.92	1.05	7.46
BaO	14.65	15.00	23.73	24.53	10.77	0.06	13.47
LOI	20.39	20.13	11.13	10.75	11.50	36.80	20.94
				ppm			
Hg	5950	6700	700	785	265	< 5	2520
Ag				630			
As				5540			
Bi				49			
Cd				1250			
Ga				65			
Ge				46			
In				3.2			
Mo				192			
Sb				1750			
Se				< 1			
Te				17.4			
Tl				62			

Fe_2O_3*: Total Fe determined as Fe_2O_3

LASCHEK, D.: Forschungsfahrt Sonne 41, HYMAS I, 18. 1. 1986-28. 4. 1986, Fahrtbericht I. Fahrtabschnitt, 1-331, Karlsruhe 1986.

MINNITI, M. and F. F. BONAVIA: Copper-ore grade hydrothermal mineralization discovered in a seamount in the Tyrrhenian Sea (Mediterranean): is the mineralization related to porphyry-coppers or to base metal lodes? — Marine Geology, **59,** 271-282, Amsterdam 1984.

PUCHELT, H.: 17. Sulfide und Oxiderze in der Tyrrhenis. — In: D. LASCHEK: Forschungsfahrt Sonne 41, HYMAS I, 18. 1. 1986-28. 4. 1986, Fahrtbericht, I. Fahrtabschnitt, 209-222, Karlsruhe 1986.

RAMDOHR, P.: Die Erzmineralien und ihre Verwachsungen. — 4th edition, Akademie-Verlag Berlin 1975.

RAMDOHR, P.: The ore minerals and their intergrowths. — 2nd edition (International series in earths sciences, **35,** editor: D. E. INGERSON), **1-2,** Pergamon Press, Oxford, New York, Toronto, Sydney, Paris, Frankfurt 1981.

STOFFERS, P. and G. C. AMSTUTZ: Complex massive sulfides on the floor of the north Central Mediterranean Sea. — Terra cognita, **7,** 323, 1987.

Table 2. Chemical composition of hydrothermal complex massive sulfide ore samples (SO 41-181 FG) from the Palinuro Seamount

	10/2	11	12/1	12/2	13	14
			percent			
CuO	0.53	0.79	0.27	0.30	0.59	0.75
PbO	6.41	9.34	4.35	4.20	19.43	12.76
ZnO	15.24	12.31	10.21	10.35	22.11	7.35
SiO_2	0.34	0.17	0.12	0.19	0.17	0.45
TiO_2	0.01	0.01	0.01	0.02	0.01	0.02
Al_2O_3	0.36	0.78	0.66	0.45	0.37	0.65
Fe_2O_3*	33.15	19.82	23.57	23.47	13.47	21.11
MnO	0.02	0.03	0.02	0.03	0.02	0.02
CaO	0.04	0.05	0.02	0.03	0.05	0.05
Na_2O	—	1.50	0.75	—	—	1.61
K_2O	0.06	0.07	0.06	0.04	0.08	0.07
P_2O_5	0.03	0.02	—	0.01	0.01	0.01
SO_3	8.15	15.24	14.74	15.56	14.29	15.90
BaO	14.25	26.02	28.15	28.59	17.40	25.01
LOI	20.39	12.58	16.15	15.83	10.90	13.10
			ppm			
Hg	2630	960	420	455	545	360
Ag	1270			465		
As	5540			4570		
Bi	1.1			4.9		
Cd	2820			1550		
Ga	702			55		
Ge	34			20		
In	15			1.9		
Mo	78			128		
Sb	1000			525		
Se	< 1			< 1		
Te	4.2			5.3		
Tl	19			25		

Fe_2O_3*: Total Fe determined as Fe_2O_3

TUFAR, W.: Lagerstättenkundliche und erzpetrographische Untersuchungen an (sub-) rezenten komplexen massiven Sulfiderzen („Schwarze Raucher") und sulfiderzhaltigen Proben des Ostpazifischen Rückens: Fahrt „Geometep 4" — „Sonne 40", Leg 3 — Schlußbericht. — In: BUNDESANSTALT FÜR GEOWISSENSCHAFTEN UND ROHSTOFFE HANNOVER — REEDEREIGEMEINSCHAFT FORSCHUNGSSCHIFFAHRT GMBH BREMEN: Abschlußbericht SO 40 — der 4. Fahrt mit FS Sonne im Rahmen des Geometep-Programms, 223-356, Hannover 1987.

TUFAR, W.: Recent Complex Massive Sulfide Deposits ("Black Smokers") and Hydrothermal Metallogenesis at Actively Spreading Plate Boundaries in the Pacific (East Pacific Rise, Galápagos Rift): Potential Marine Mineral Resources and a Future Field of Activity for Deep-sea Mining. — Journal of Engineering, Islamic Republic of Iran, National Center for Scientific Research, **1**, No. 4, 219-241, Teheran 1988.

TUFAR, W.: Recent Complex Massive Sulfide Deposits ("Black Smokers") and Hydrothermal Metallogenesis at Actively Spreading Plate Boundaries in the Pacific (East Pacific Rise, Galápagos Rift): Potential Marine Mineral Resources and a Future Field of Activity for Deep-sea Mining. — Second Mining Symposium Iran, Kerman 1988, Ministry of Mines and Metals, University of Teheran, **3**, Proceedings, 1-47, Teheran 1989.

TUFAR, W.: Complex Massive Sulfide Formation in the Tyrrhenian Sea (Mediterranean, Italy). — 8th IAGOD Symposium in conjunction with International Conference on Mineral Deposit Modelling, Program with Abstracts, A 64, Ottawa 1990 a.

TUFAR, W.: Modern Hydrothermal Activity, Formation of Complex Massive Sulfide Deposits and Associated Vent Communities in the Manus Back-Arc Basin (Bismarck Sea, Papua New Guinea). — Mitt. österr. geol. Ges., **82**, 1989, 183-210, Vienna 1990 b.

Table 3. Chemical composition of hydrothermal complex massive sulfide ore samples (SO 41-181 FG) from the Palinuro Seamount (after H. PUCHELT, 1986)

	5/1	5/2	6	7/1	7/2	7/3	8/1	8/2
					percent			
Fe	35.20	18.90	15.30	26.90	14.90	3.26	4.80	12.00
Zn	2.99	15.30	11.30	17.80	28.20	3.48	27.20	23.90
Pb	4.33	4.92	12.60	2.51	10.90	1.04	7.76	12.50
Cu	0.21	0.32	0.52	0.33	0.06	0.40	1.21	0.61
Ba	3.49	15.46	20.06	7.68	7.20	48.02	12.16	13.45
					ppm			
Ag	200	220	350	70	40	100	250	300
As	4000	3400	3800	4900	3400	1800	4800	4500
Au	0.52	0.46	7.08	3.52	2.50	1.14	5.39	3.62
Br	6.60	7.80	10.30	2.40	5.70	11.90	10.30	5.40
Cd	390	2110	550	1410	1620	510	990	1080
Co	7.17	4.94	3.97	12.98	10.54	3.05	21.77	18.52
Cr	23.10	< 45.00	< 31.00	26.40	31.50	< 23.00	—	—
Ga	17	121	22	29	< 12	71	28	31
Hg	1200	6400	1400	760	468	554	230	399
In	—	26	13	< 19	—	27	< 20	17
Mo	< 39	99	98	113	76	< 35	147	77
La	0.97	2.12	4.66	3.80	1.60	8.54	3.35	2.85
Sb	505	2000	938	292	337	200	1300	933
Sc	0.18	< 0.3	< 0.2	< 0.3	< 0.3	< 0.1	< 0.3	< 0.4
Se	7.10	—	19.30	< 12	—	< 9	—	—
Ta	—	0.29	75	62	—	< 43	—	< 70
Th	1.63	< 3	< 2	1.18	—	< 1	—	—
W	4.50	3.10	2.60	11.80	0.90	6.20	4.40	2.90
U	—	1.80	1.60	2.00	—	2.70	5.00	3.00

TUFAR, W.: Hydrothermale Aktivität auf dem Meeresboden — 3 Ostpazifischer Rücken, Galápagos-Rift, Rotes Meer, Tyrrhenisches Meer. — Geol. Jb., **D 93**, „Forschungsschiff Sonne — 50 Fahrten im Dienst der geowissenschaftlichen Meeresforschung"-Commemorative Volume, 140-153, 169-193, Hannover 1991.

TUFAR, W., H. Gundlach and V. Marchig: Zur Erzparagenese rezenter Sulfid-Vorkommen aus dem südlichen Pazifik. — Mitt. österr. geol. Ges., **77**, 1984, 185-245, Wien 1984.

TUFAR, W., H. Gundlach and V. Marchig: Ore Paragenesis of Recent Sulfide Formations from the East Pacific Rise. — Monograph Series on Mineral Deposits, **25**, H.-J. Schneider-Commemorative Volume (editor: K. GERMAN), 75-93, Berlin — Stuttgart 1985.

TUFAR, W., E. TUFAR, and J. LANGE: Zur Paragenese von rezenten Hydrothermalprodukten an der Cocos-Nazca-Plattengrenze bei 85° 50' W: Komplexe massive Sulfiderze („Schwarze Raucher"), Basaltvererzungen und -Alterationen, postgenetische Veränderungen. — Included in: LANGE, J. and PROBST, U.: Schlußbericht Mineralische Rohstoffe — GARIMAS 1 — Galápagos Rift Massivsulfide. — Preussag AG Meerestechnik, Schlußbericht Bundesminister für Forschung und Technologie, 1-34, Hannover 1986 a.

TUFAR, W., E. TUFAR, and J. LANGE: Ore paragenesis of recent hydrothermal deposits at the Cocos-Nazca plate boundary (Galápagos Rift) at 85° 51' and 85° 55' W: complex massive sulfide mineralizations, non-sulfidic mineralizations and mineralized basalts. — Geol. Rdsch. **75**, No. 3, Hans Cloos-Commemorative Volume, 829-861, Stuttgart 1986 b.

TUFAR, W., H. PUCHELT, D. LASCHEK and J. LANGE: Zur Erzparagenese von komplexem Sulfiderz aus dem Tyrrhenischen Meer. — Abschlußbericht „HYMAS I", 1-41, 1987.

Table 4. Chemical composition of hydrothermal complex massive sulfide ore samples (SO 41-181 FG) from the Palinuro Seamount (after H. PUCHELT, 1986)

	9/1	9/2	10	12/1	12/3	13	14
				percent			
Fe	3.57	4.87	16.80	32.90	15.30	8.68	13.30
Zn	23.70	26.90	19.40	11.00	19.30	21.40	16.90
Pb	13.30	14.50	10.10	10.40	3.74	9.24	11.80
Cu	1.04	0.79	0.29	0.35	0.37	0.54	0.46
Ba	21.79	16.20	13.88	7.50	20.85	19.29	17.31
				ppm			
Ag	400	380	460	240	350	360	310
As	4100	3600	2200	2600	2100	2500	3100
Au	5.67	4.91	1.04	2.28	3.99	4.32	4.41
Br	11.70	11.80	2.20	18.80	2.90	15.20	13.10
Cd	1230	1480	1560	1050	1580	1260	990
Co	12.72	15.14	4.16	4.57	4.71	5.85	6.67
Cr	—	—	36.50	24.50	30.00	36.10	28.50
Ga	44	36	77	60	41	16	18
Hg	575	448	4800	1200	1200	633	650
In	—	16	22	27	20	< 25	< 18
Mo	178	93	53	21	38	76	91
La	10.00	6.17	2.56	2.51	10.10	7.27	4.53
Sb	996	1200	730	196	300	550	711
Sc	< 0.3	< 0.3	< 0.3	< 0.2	0.15	< 0.3	< 0.3
Se	17.20	< 16	—	17.00	—	< 15	—
Ta	—	37	0.19	< 65	37	< 71	< 50
Th	1.06	1.09	< 2.0	< 2.0	—	1.30	—
W	4.80	4.30	3.20	3.30	5.40	2.10	2.00
U	4.40	1.30	—	1.70	0.70	2.70	1.20

WARD, D. M., R. WELLER, J. SHIEA, R. W. CASTENHOLZ and Y. COHEN: Hot Spring Microbial Mats: Anoxygenic and Oxygenic Mats of Possible Evolutionary Significance. — In: COHEN, Y. and E. ROSENBERG (Editors): Microbial Mats — Physiological Ecology of Benthic Microbial Communities, 3-15, Washington (D. C.) 1989.